



NTNU – Trondheim
Norwegian University of
Science and Technology

Effect of Barriers in Air Insulated Rod-Plane Gaps

Jonathan S Jørstad

Master of Energy and Environmental Engineering

Submission date: June 2012

Supervisor: Frank Mauseth, ELKRAFT

Co-supervisor: Atle Pedersen, SINTEF

Norwegian University of Science and Technology
Department of Electric Power Engineering

Problem Description

Due to environmental issues it is a trend today to avoid climate gases like SF₆. Thus, the use of air as insulation gas has lately been of high focus to producers of high voltage equipment. The withstand voltage of air is lower than SF₆, and a challenge for electrical engineers is to make compact air insulated equipment. It is common to use barriers in the design to increase the path of the streamer and thus increasing the withstand voltage.

During the design process it is common to use Finite Element Analysis to calculate the electrostatic field strength on the different components in the equipment. However, knowing the electrostatic field distribution is not sufficient to predict the withstand voltage. It is also necessary to model the discharge processes including inception and propagation of streamers.

The main topic of the proposed project work will be the study of initiation and propagation of streamers in air insulated rod-plane gaps with insulating barriers. The work will consist of both laboratory measurements and electromagnetic simulations of breakdown in an electrode gap with barriers. Comparison of the results will be used to make design criteria for predicting the withstand voltage of electrode gaps with barriers.

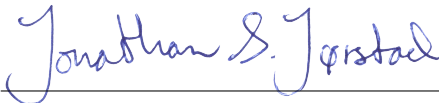
This project will be done in cooperation with ABB Corporate Research in Daetwill, Switzerland.

Preface

The purpose of the experiments conducted in this Master's thesis is to predict and explain the change in breakdown voltage when insulating barriers are introduced in a rod-plane gap arrangement. This report contains some theory on the streamer mechanism and the barrier effects as well as a summary of the results presented in tables and figures. Explanations of the observed phenomena are discussed.

I would like to express my thanks to my supervisors, Associate Professor Frank Mauseth of the Norwegian University of Science and Technology and Research Scientist Atle Pedersen at SINTEF Energy Research for their excellent support and guidance through the spring semester. I would also like to thank Dr. Andreas Blaszczyk, Senior Scientist at ABB Corporate Research, for his valuable input concerning this thesis.

Trondheim, 22nd June, 2012



Jonathan Skramstad Jørstad

Abstract

The purpose of the experiments conducted in this Master's thesis is to predict and explain the change in breakdown voltage when insulating barriers are introduced in a rod-plane gap arrangement. The experiments have been conducted with positive lightning impulse voltage, using the up and down method to determine the 50 % breakdown voltage. A cylindrical rod with rounded tip and radius 3.5 mm was used as the high voltage electrode above a grounded plane electrode. The polycarbonate barriers used were 1 mm thick and of different sizes (4x4 cm, 6x6 cm, 8x8 cm, 16x16 cm, 30x30 cm and 40x40 cm). They were placed at various positions in an 80 mm rod-plane gap to find the optimal combination.

The results show that the breakdown voltage of the gap can be increased by the use of barriers, strongly dependent upon their size and position. The largest barrier offered the highest breakdown voltage with an increase of 98.0 % versus the barrier-less rod-plane gap. For the two largest barriers, the optimal position was found to be in the upper part of the gap, 0 – 10 mm from the high voltage rod tip. The four smaller barriers perform their best around 20 mm from the tip. It has been suggested in literature that the optimal position is in the range 12 – 24 mm for this gap [8], where the breakdown voltage can be over tripled.

It has been discovered that placing the smallest barriers close to the high voltage rod tip drops the breakdown voltage to levels below that of the barrier-less gap. A suggested explanation is the strong tangential field present on the barrier surface under these conditions, quickly building up charge on the barrier and leading to breakdown. Streamer inception on the underside of the barrier has not been observed despite the high field strength directly under the rod tip. This is possibly caused by the slightly higher field on the upper side of the barrier, leading to streamer inception which weakens the field under the rod tip. As the barrier size is increased, the voltage drop in the longer streamer path is the dominating factor behind the rise in breakdown voltage. It is recommended to employ barriers of considerable size, preferably having a cross-sectional length of twice the gap distance or longer, to ensure satisfactory breakdown performance improvement. An empirical equation for predicting breakdown voltage in barrier insulated rod-plane gaps has been constructed on the basis of the conducted experiments.

Sammendrag

Hensikten med de utførte forsøkene i denne masteroppgaven er å kunne forutsi og forklare endringen i overslagsspenning når barrierer benyttes som isolasjon i stang-plate-gap. Forsøkene er utført med positiv lynimpuls der opp og ned-metoden er benyttet for å fastslå 50 %-overslagsspenning. En sylinderformet stang med avrundet tupp og radius 3,5 mm er benyttet som høyspentelektrode over en flat jordelektrode. De benyttede barrierene av polykarbonat er 1 mm tykke og av ulike størrelser (4x4 cm, 6x6 cm, 8x8 cm, 16x16 cm, 30x30 cm og 40x40 cm). De ble plassert på ulike posisjoner i et 80 mm stort stang-plate-gap.

Resultatene viser at overslagsspenningen i gapet kan økes gjennom bruk av barrierer, sterkt avhengig av barrierenes størrelse og posisjon. Den største barrieren ga den høyeste overslagsspenningen, en økning på 98.0 % i forhold til stang-plate-gapet uten barriere. Optimal plassering for de to største barrierene er i den øvre delen av gapet, 0 – 10 mm fra den høyspente stangelektroden. De fire mindre barrierene ga høyest overslagsspenning rundt 20 mm fra stangelektroden. I litteraturen er det argumentert for en optimal plassering som tilsvarer 12 – 24 mm for dette gapet [8], der en tredobling av overslagsspenningen har blitt oppnådd.

En plassering av de mindre barrierene nærme den høyspente elektroden har vist seg å gi en lavere overslagsspenning enn for gapet uten barriere. En forklaring på dette kan være det sterke tangentielle feltet på barriereoverflaten i disse tilfellene. Feltet lader barrieren raskt opp og kan bidra til overslag. Tenning av streamere på undersiden av barrieren har ikke blitt observert på tross av at feltet er meget sterkt rett under stangtuppen. Dette skyldes muligens at det noe sterkere feltet på oversiden leder til tenning der, noe som svekker feltet under stangtuppen. Etter hvert som barrierestørrelsen økes er spenningsfallet i streameren den viktigste faktoren bak den høyere overslagsspenningen. Det anbefales å benytte barrierer av betydelig størrelse i forhold til gaplengden for å sikre tilfredsstillende økning av overslagsspenning, gjerne med en tverrsnittslengde dobbelt så stor som gapet eller lengre. En empirisk formel for å predikere overslagsspenning i barriere-isolerte stang-plate-gap er konstruert på bakgrunn av de utførte eksperimentene.

Contents

1	Introduction	1
2	Theory of Breakdown in Gases	3
2.1	Townsend Mechanism	3
2.2	Streamer Mechanism	4
2.2.1	The Streamer Path	5
2.3	The Barrier Effect	7
2.4	Breakdown Voltage As a Stochastic Variable	8
3	Methods and Instrumentation	11
3.1	Experimental Set-Up	11
3.1.1	Impulse Voltage Generator	11
3.1.2	The Rod-Plane Gap	13
3.1.3	Measuring Circuit	14
3.1.4	Photography	15
3.1.5	Air Density Correction	15
3.1.6	Calibration of the Experimental Set-Up	16
3.2	Experimental Method	17
3.2.1	Up and Down Method	19
3.3	Field Calculation Using COMSOL	20
3.4	Streamer Inception Voltage Calculation Using Matlab	22
4	Results	23
4.1	Breakdown Voltage of Rod-Plane Gap	23
4.2	Breakdown Voltage of Rod-Plane Gap with Barrier	24
4.3	Streamer Photography	28
4.4	Electric Field Simulation and Inception Voltage Calculation	32
5	Discussion	37
5.1	Rod-Plane Gap	37
5.2	Rod-Plane Gap with Barrier	38
5.3	Sources of Error	41
6	Conclusion	43
7	Further Work	45
8	References	47
	Appendix A Matlab Source Code	49

1 Introduction

There is a desire in the market for compact high voltage equipment, e.g. in the wind industry. This can be achieved by using SF₆ as the insulating medium. However, SF₆ is a greenhouse gas and the increasing environmental focus makes it necessary to consider other media, such as air.

The withstand and breakdown voltages of air are lower than of SF₆, so in order to keep a compact design, insulating barriers can be used to increase breakdown voltage to the required level. The withstand increase is a result of the extension of the streamer path needed to short the electrodes. The barrier effect is discussed in literature and it is claimed that the breakdown voltage can be tripled under optimal conditions [8]. The aim of this Master's thesis is to determine the expected increase in breakdown voltage and to explain the mechanisms behind this and other effects observed.

The problems are addressed by conducting lightning impulse voltage tests on a rod-plane gap. Insulating barriers of varying size are inserted at different positions in the gap to find the optimal combination. Breakdown voltage levels are determined with the up and down method. Its advantage of requiring few shots has made this method popular, but it must be carefully applied in order to get reliable results. Electric field distributions are calculated with finite element analysis in COMSOL so that observed streamer paths and breakdown voltage levels may be explained. Field calculations are done with simplifications such as assumption of uniform charge distribution on the barrier surface. The experiments are limited to square polycarbonate barriers of size up to 40x40 cm. The measurements are corrected for pressure changes, but standard humidity and temperature is assumed. In addition to determining the breakdown voltage levels, photographs of the rod-plane gap are taken during lightning impulses resulting in breakdown and withstand to observe the streamer behaviour.

In the following sections, relevant fundamental theory on the subject is presented and the experimental set-up explained. The results are presented in tabular and graphical form and discussed in relation to theory.

2 Theory of Breakdown in Gases

2.1 Townsend Mechanism

The Townsend theory explains the mechanism of breakdown in gases under certain conditions. The below-mentioned theory is compiled from [1], [2] and [3].

Electrons exposed to an electric field are accelerated in the opposite direction of the field, towards the anode (the positive electrode). The field exerts work on the electron as defined by Eq.(1), where e is the electron charge and x is the distance travelled along a field line.

$$W = eEx = \frac{1}{2}mv^2 \quad (1)$$

The high velocity electron will have a certain probability of colliding with molecules in the insulating gas. In an inelastic collision energy is transferred to the molecule. This enables the molecule to be ionized and give up an electron, which in turn will be accelerated by the electric field and maybe cause another ionizing collision. The first Townsend coefficient α gives the probability that one electron will cause an ionizing collision per unit length, liberating an electron. With higher pressure, the probability of collision is increased. The kinetic energy of the electron is proportional with the applied field, and the coefficient α is therefore a function of the fraction $\frac{E}{p}$. The number of collisions is proportional to the pressure.

The second Townsend coefficient γ gives the probability of liberation of secondary electrons. The secondary electrons can for instance originate from the cathode (the negative electrode), being triggered by positive ions impinging on the cathode. In this case the ion must release two electrons, one to neutralize the ion charge and one that is ejected as a secondary electron. This is the main secondary process in the Townsend mechanism, and it is also a function of the electric field strength and the gas pressure. Photo emission may also contribute to secondary electrons. The released electrons are accelerated towards the anode in an avalanche and can possibly cause breakdown.

$$I = I_0 \frac{e^{(\alpha-\eta)d}}{1 - \frac{\gamma\alpha}{\alpha-\eta}(e^{(\alpha-\eta)d} - 1)} \quad (2)$$

In electronegative gases, the molecules or atoms are able to absorb electrons to fill their outer shell. The probability that an electron is attached to such a molecule per unit length is given by the attachment coefficient η . This process will hamper the flow of electrons produced by the above-mentioned processes. Taking all these processes into account, the current at the anode can be described as in Eq.(2) [2]. The equation shows that breakdown will happen if the denominator goes to zero, which defines the Townsend breakdown criterion.

2.2 Streamer Mechanism

Breakdown has been observed to occur at substantially shorter time lags than proposed by the Townsend mechanism. Around 1940, the theory on streamers were proposed by Raether, Meek and Loeb, predicting breakdown caused by a single electron avalanche [3].

When the number of electrons in the avalanche reaches a critical size N_{cr} the avalanche becomes self-propagating. This is caused by the enhanced field in front of the avalanche head, leading to intense ionization and excitation of gas particles [1]. The emitted photons, travelling at the speed of light, can release additional electrons and lead to conductive channels across the gap.

The streamer inception criterion is given in Eq.(3). α_{eff} defines the combined effect of the Townsend coefficients and the attachment coefficient and is a function of the electric field strength. The integration path Γ follows the projected streamer path along a field line where $\alpha_{eff} > 0$. The path starts at the point of maximum field strength and ends where the critical field value of $E_{cr} = 2.5$ kV/mm is reached [4], called the inception field strength. Beyond this point $\alpha_{eff} < 0$. In the event that the maximum field strength does not occur on the electrode, but on for instance an insulator, electrodeless inception can occur at this point. From here, the streamer can simultaneously propagate towards both electrodes [5].

$$\int_{\Gamma} \alpha_{eff} dx = \ln(N_{cr}) \approx \ln(10^8) \quad (3)$$

For strongly inhomogeneous electric fields the critical number of electrons is $N_{cr} \approx 10^8$ [5]. By calculating the number of electrons, the inception voltage U_{si} can be determined iteratively, increasing the voltage in each iteration until the critical number of electrons is reached. The calculation of α_{eff} per mm is shown in Eq.(4) [6] which is valid on the interval $2.588 < \frac{E}{p} < 7.943$ kV/mm · bar. The electric field distribution must be known for instance from computer simulations.

$$\frac{\alpha'_{eff}}{p} = 1.6053 \text{ mm} \cdot \text{bar}/\text{kV}^2 \cdot \left[\frac{E}{p} - 2.165 \text{ kV}/\text{mm} \cdot \text{bar} \right]^2 - 0.2873 / \text{mm} \cdot \text{bar} \quad (4)$$

In homogeneous or weakly inhomogeneous fields, streamer inception will immediately lead to breakdown [5]. In Figure 1 it can be seen that the slope of the inception voltage in this region is 2.6 kV/mm. After the transition to a strongly inhomogeneous field, denoted by the point P in the figure, withstand voltage U_W (red line) is no longer determined by the inception voltage. In this case there will be a small time lag before a possible breakdown can occur.

$$U_W = U_0 + d \cdot E_{st} \quad (5)$$

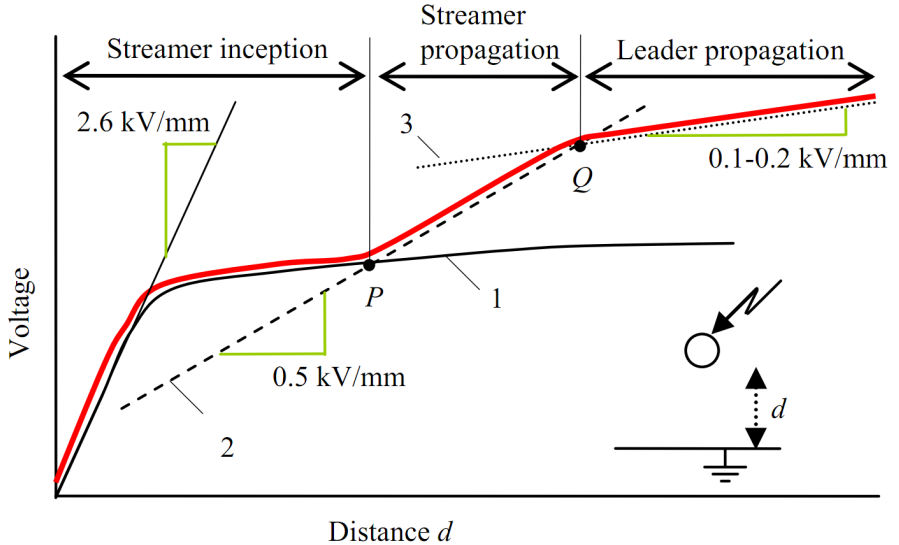


Figure 1: Withstand voltage with respect to field homogeneity [7]

The applied voltage must be of a certain level to allow for streamer propagation to take place. If the voltage is too low, the streamer will not advance and there will be no breakdown. The lowest impulse voltage needed for streamer propagation is given by Eq.(5) [7]. This equation is represented by a dashed line in Figure 1 and defines the withstand in inhomogeneous electric fields, for instance in a rod-plane gap. Hence this equation is not valid for small gap distances where the field distribution is more uniform. U_0 in Eq.(5) is the voltage needed for the streamer head to cause breakdown, the value used here is 24.4 kV [4]. In [7] it is more loosely defined in the region $U_0 \approx 20 - 30$ kV. For positive impulse voltages the streamer propagation field is $E_{st} = 0.54$ kV/mm [7], which is equal to the internal field strength of the streamer. A much higher field is necessary for negative streamers, up to $E_{st} = 1.2$ kV/mm, requiring a significantly higher voltage compared to positive streamers. The attention should therefore be paid to the latter of the two. Point Q in Figure 1 marks the transition to the leader region. The gap must be quite large before leader transition can occur, around 2 m. The voltage drop in a leader is lower than that of the streamer and it can therefore extend over long distances.

2.2.1 The Streamer Path

Predicting the streamer path is of importance in regard to estimating the breakdown voltage. As shown in Figure 1 and in Eq.(5) the withstand voltage increases with the gap distance. In the streamer propagation region in the figure, the relationship is linear and given by the internal field strength of the streamer of 0.54 kV/mm.

It is often assumed that the streamer will start at the point with the highest field strength and then propagate along an electric field line $-\vec{\nabla}V$. It has been observed that streamer paths systematically deviate from this assumption [5]. The mentioned streamer propagation field is the minimum field that can support streamer propagation. If the streamer propagates into a field lower than this, it will deflect or stop. One attempt at streamer path modelling is shown in Eq.(6) [5]. The model suggests that the streamer follows the field line until the field strength is too low, then the streamer is deflected and follows the edge of this region towards higher field strength. This is achieved in the equation by setting $A(E < 0.54 \text{ kV/mm}) = 0$. The streamer will propagate until it finds the opposite electrode or stop if $\vec{\nabla} \cdot \vec{E}^2$ is parallel to \vec{E} .

$$\vec{v}_s = A(E) \cdot \vec{E} + B \cdot \vec{\nabla} \cdot \vec{E}^2 \quad (6)$$

Another suggestion is that the streamer path will follow the maximum field [7], even if this means crossing field lines. The path can be found by identifying the point of maximum field strength at each equipotential curve, and connecting these points.

When introducing an obstacle in the gap, such as an insulating barrier, the streamer must either penetrate the barrier or find a path around it. In either case the withstand voltage increases, a beneficial effect which can be utilized when a compact design is desired.

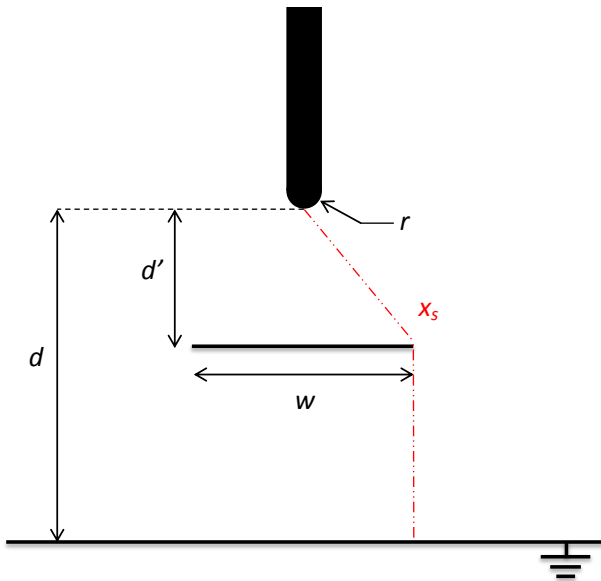


Figure 2: Rod-plane gap with insulating barrier

Consider the gap arrangement in Figure 2. The figure illustrates a conventional rod-plane gap, for instance air-insulated. Assuming that the streamer will not penetrate the barrier, the shortest distance between the rod tip and the grounded plane electrode is called x_s and indicated by a red dashed line in the figure. The length of x_s is calculated in Eq.(7). A hypothesis to be tested in this thesis is whether introducing a barrier in the gap gives similar breakdown performance as a barrier-less gap with gap distance equal to x_s . Assuming this can be done, the new withstand voltage can be found from Eq.(5), with x_s replacing d . This approach to approximating the withstand voltage does not take into account any barrier effects such as surface charge accumulated on the barrier, influencing the electric field. If withstand voltage for the gap without the barrier is known from experiments, the new withstand voltage can be found with Eq.(8).

$$x_s = d - d' + \sqrt{d'^2 + \left(\frac{w}{2}\right)^2} \quad (7)$$

$$U_{\text{with barrier}} = U_{\text{no barrier}} + (x_s - d) \cdot E_{st} \quad (8)$$

2.3 The Barrier Effect

Introducing a barrier in a rod-plane gap as in Figure 2 will not affect the background electric field severely, but the effects of obstructing charge carriers in the gap can be substantial. By increasing the applied voltage on the rod electrode there will at a certain point be partial discharges. The electric field will accelerate electrons in the direction of the rod (assuming a positive applied voltage). Positive ions left behind will be accelerated towards the ground electrode. As the positive charges accumulate on the obstructive barrier, the electric field will be weakened between the barrier and the rod tip, increasing withstand voltage. Because of the barrier surface charge, the electric potential on the barrier can be assumed equal to that of the rod [8]. Given time, the positive ions will be uniformly distributed and contribute to a more uniform electric field beneath the barrier, also increasing the withstand [9].

In a rod-plane gap, the optimal position of the barrier is such that $\frac{d'}{d} = 0.2$ [9], or at least in the region $\frac{d'}{d} = 0.15 - 0.3$, where the breakdown voltage can be over tripled with large insulating barriers[8]. Smaller barriers give a lower increase [10]. Moving the barrier close to the rod or the plane electrode can decrease the breakdown voltage to the same level as a gap without the barrier [8]. This is not in accordance with the assumption of linearly increasing withstand voltage with the shortest streamer path distance presented in Eq.(7). In fact, the experimental results of [11] shows a trend where a barrier position of $d' = 0$ mm decreases the breakdown voltage below the original level without the barrier.

2.4 Breakdown Voltage As a Stochastic Variable

The phenomena of breakdown is a stochastic process. Breakdown will not always occur at the exact same voltage level due to the random property of events such as collision between electrons and molecules and electron detachment. When discussing the breakdown voltage, one often refers to the voltage that leads to breakdown with a 50 % probability, U_{50} .

The most used probability distributions for breakdown voltages are the normal (Gaussian) and Weibull distributions. By experience, the normal distribution fits the experimental data well in the area around the 50 % value [2]. Near the tails it is less accurate. An advantage of the Weibull distribution is that it can be adapted more accurately to the experimental data. The theory on statistics and probability in this section is compiled from the textbook of Walpole et al. on the subject [12].

$$\bar{X} = \frac{1}{n} \sum_{i=1}^n x_i \quad (9)$$

$$Z = \frac{\bar{X} - \mu}{\sigma/\sqrt{n}} \quad (10)$$

From the experimental data (the different values x_i of the stochastic variable X) the true mean μ can be estimated and a confidence interval constructed. The central limit theorem states that the variable Z in Eq.(10) follows the standard normal distribution when the sample size n approaches infinity. This approximation is generally good when $n \geq 30$, for smaller sample sizes the approximation can still be used if the distribution of X is close to the normal distribution. Using existing tables on quantiles of the standard normal distribution, assuming that the Gaussian distribution is indeed applicable, a two sided confidence interval is constructed in Eq.(11). By using the transformation of Eq.(10) the $100(1 - \alpha)$ % confidence interval limits are as given in Eq.(12).

$$P(-z_{\alpha/2} < Z < z_{\alpha/2}) = 1 - \alpha \quad (11)$$

$$\bar{x} - z_{\alpha/2} \frac{\sigma}{\sqrt{n}} < \mu < \bar{x} + z_{\alpha/2} \frac{\sigma}{\sqrt{n}} \quad (12)$$

$$\bar{x} - t_{\alpha/2} \frac{s}{\sqrt{n}} < \mu < \bar{x} + t_{\alpha/2} \frac{s}{\sqrt{n}} \quad (13)$$

The use of the normal distribution here assumes that the standard deviation σ of the experiment observations is known. This is usually not the case, and it is therefore estimated instead. Under these circumstances it is more correct to use the

student t -distribution rather than the standard normal distribution. The interval will then take the form of Eq.(13), where s is an estimate of the standard deviation σ and the value of $t_{\alpha/2}$ is found in statistical tables [13]. An estimator suitable for the experiments in question will be given in section 3.2.1 about the up and down method.

Linear Regression

It can often be productive to employ linear regression to a set of data to quantify the trend for comparison with theory or hypotheses. The method of least squares is a commonly used method to estimate the parameters α and β of Eq.(14), the true linear trend where ϵ represents random error. An estimation $\hat{y}(x)$ of the true line is done by calculating the estimators a and b of Eqs.(17) and (16), respectively, where \bar{y} and \bar{x} are mean values of the measurements. Derivation of the estimators is beyond the scope of this thesis.

$$Y = \alpha + \beta x + \epsilon \quad (14)$$

$$\hat{y} = a + bx \quad (15)$$

$$b = \frac{\sum_{i=1}^n (x_i - \bar{x})(y_i - \bar{y})}{\sum_{i=1}^n (x_i - \bar{x})^2} \quad (16)$$

$$a = \bar{y} - b\bar{x} \quad (17)$$

As the estimators are products of measured values that can be more or less accurate, it can be valuable to construct confidence intervals to determine this uncertainty. A $100(1 - \alpha)$ % confidence interval for the slope β is given in Eq.(19).

$$\frac{s^2}{S_{xx}} = \frac{\sum_{i=1}^n (y_i - \bar{y})^2 - b \sum_{i=1}^n (x_i - \bar{x})(y_i - \bar{y})}{(n - 2) \sum_{i=1}^n (x_i - \bar{x})^2} \quad (18)$$

$$b - t_{\alpha/2} \frac{s}{\sqrt{S_{xx}}} < \beta < b + t_{\alpha/2} \frac{s}{\sqrt{S_{xx}}} \quad (19)$$

3 Methods and Instrumentation

3.1 Experimental Set-Up

3.1.1 Impulse Voltage Generator

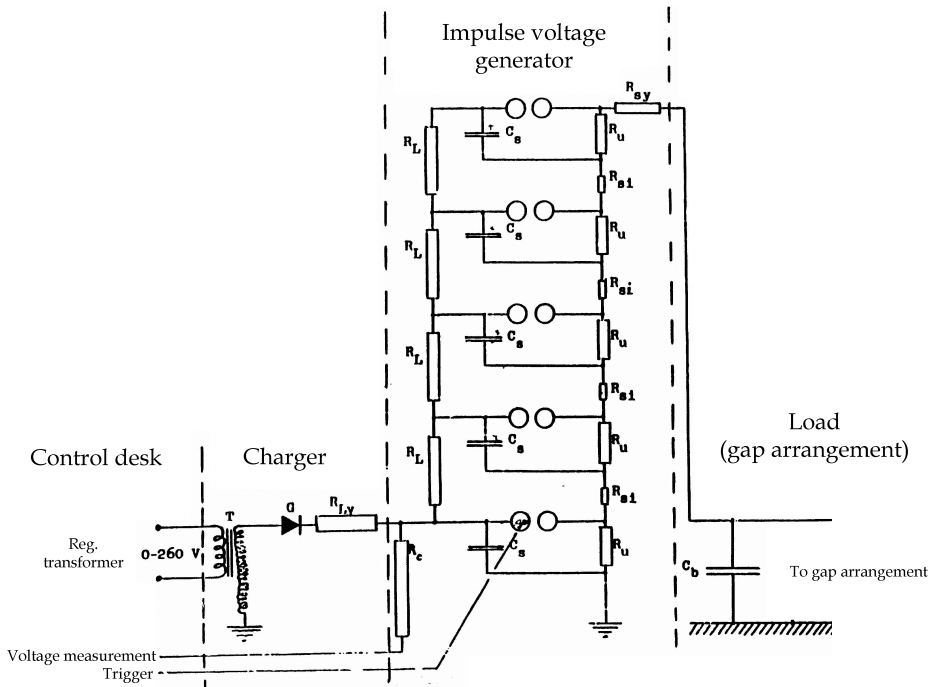


Figure 3: Impulse voltage generator [14]

The purpose of the set-up is to provide an amplitude controlled lightning impulse voltage for the rod-plane gap arrangement to generate breakdown and determine the 50 % breakdown voltage.

The experiments were conducted in a student high voltage laboratory at NTNU (E-152). The main components of the set-up were the following:

- Control desk from which the charging voltage as well as sphere gap breakdown voltage were adjusted
- Transformer used to charge capacitors
- Rectifier used to rectify capacitor charging voltage
- Five impulse capacitors
- Sphere gaps to connect the capacitors in series

- Discharge capacitor
- Rod-plane gap
- Voltage divider
- Measurement circuit including oscilloscope

A sketch of the impulse voltage generator can be found in Figure 3. From the control desk, the charging voltage for the capacitors could be controlled and charging current monitored. Higher voltage will charge the capacitors faster. The sphere gap distance was also controlled from the desk. The purpose of the sphere gaps was to change the configuration of the capacitors from parallel to series. This allows a voltage of five times the charging voltage to be discharged into the test object. The rod-plane gap and the measuring circuit were connected to the right terminals in the Figure 3. The impulse voltage generator consists of the following components:

T Transformer

G Rectifier

R_{LY} Charging resistor 1 m Ω

R_F Resistor for voltage measurement 160 m Ω

R_L Charging resistor 30 k Ω

R_U Discharge resistor 326 Ω

R_{Sj} Series resistor 55 Ω

R_{SY} Series resistor 570 Ω

C_S Impulse capacitor 0.25 μ F

C_D Discharge capacitor 560 pF

Measurements of the applied voltage pulse show that the front time is 1.29 μ s and the time to half-value 55.1 μ s. This is close to the standard standard 1.2/50 lightning impulse voltage defined in IEC60060-1. A sample impulse voltage from this particular set up is presented in Figure 4.

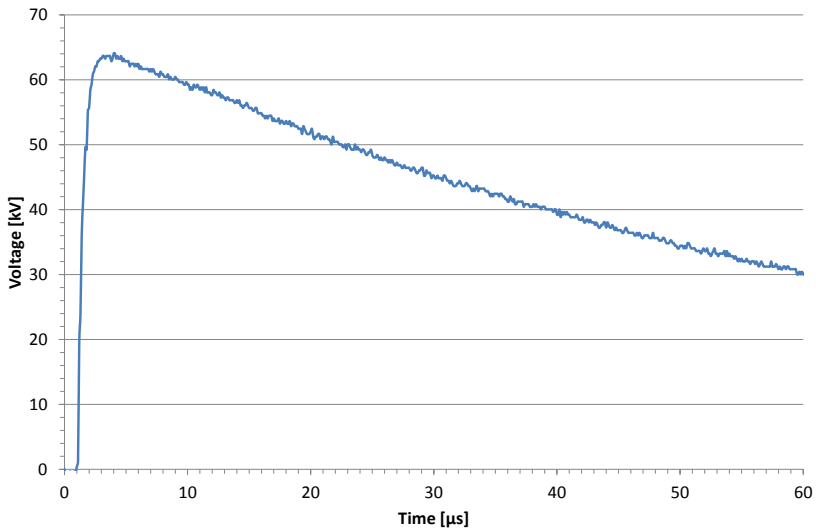


Figure 4: Sample impulse voltage

3.1.2 The Rod-Plane Gap

A custom gap arrangement was built to conduct the experiment. It is depicted in Figure 8 and measures 30x30x60 cm. This arrangement does not include a plane electrode and must therefore be placed on one, like in the picture.

The tubular framework is made of compressed cardboard, the same goes for the bottom square frame. The upper plate and the rod support are made of plastic. The rod has a diameter of 7 mm and is made of aluminium. The tip is rounded with the same diameter. For breakdown tests with barriers, six polycarbonate barriers were made by the shapes of Figure 5. They measure 4x4 cm, 6x6 cm, 8x8 cm, 16x16 cm, 30x30 cm and 40x40 cm with a thickness of 1 mm. Holes were drilled in the corners to allow for mid-air suspension using rubber bands attached to the tubular supports. The larger barriers of size 16x16 cm and upwards were suspended by a standard type of fishing line. The rod was connected to the impulse voltage generator in Figure 3 by wire. Note that the largest barrier did not fit in between the supports of the rod-plane gap and was therefore adapted by cutting away the corners. One may expect this to lower the breakdown voltage, even though the distance from the centre to one of the cut-out corners is longer than $\frac{40 \text{ mm}}{2}$.

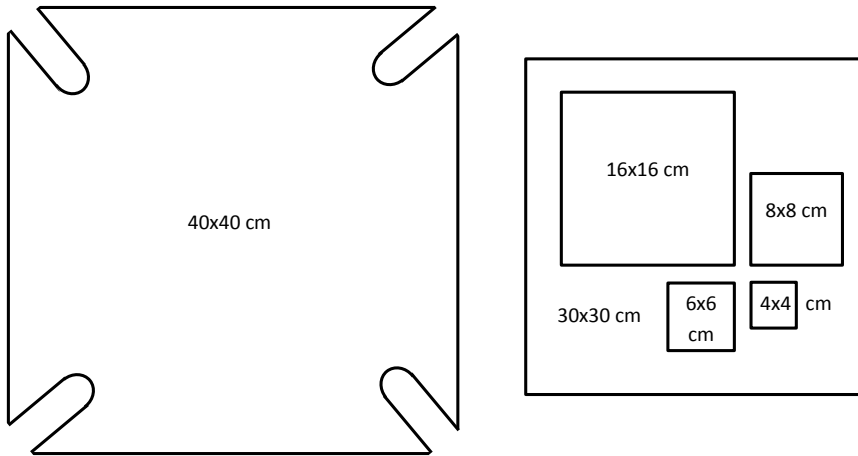


Figure 5: Barrier sizes

3.1.3 Measuring Circuit

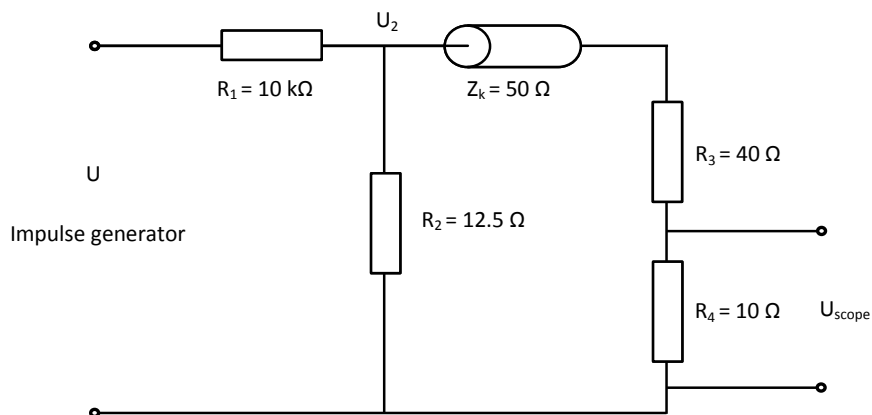


Figure 6: Measuring circuit

The voltage over the rod-plane gap was measured with an oscilloscope. Because of the high voltage, several voltage dividers were used. The configuration of the measuring circuit can be seen in Figure 6, where the left side is connected to the gap and the right side to the oscilloscope. The impedance values are given below.

R_1 10 k Ω

R_2 12.5 Ω

Z_k 50 Ω characteristic impedance

R_3 40 Ω

R_4 10 Ω

Given the measured voltage U_{scope} , the true gap voltage U can be calculated as follows:

$$U_2 = \frac{U \cdot R_2 || Z_k}{R_1 + R_2 || Z_k} \quad (20)$$

$$U_{scope} = U \cdot \frac{R_4}{R_3 + R_4} \cdot \frac{R_2 || Z_k}{R_1 + R_2 || Z_k} \quad (21)$$

$$U = 5005 \cdot U_{scope} \quad (22)$$

3.1.4 Photography

Photographs were taken of lightning impulse voltages both resulting in breakdown and withstand. The bright breakdown channel allowed for the use of a standard DSLR camera to be used in these situations. The streamers present in the gap during a lightning impulse where a breakdown does not develop are only barely visible. For this purpose, a Phantom v606 high speed camera was used in addition to a Lambert Instruments II25 image intensifier to be able to depict the streamers. The camera was connected to a computer for image triggering, acquisition and storage.

3.1.5 Air Density Correction

To be comparable with theoretical values and other experiments the measured voltages have been corrected for air density. This is done according to Eq.(23), where U_{d0} is the voltage at standard conditions. The air density is given by Eq.(24) [1]. For values of δ in the interval 0.95 – 1.05, $k_d = \delta$. It has been assumed that the temperature was constant and equal to T_0 during the experiment.

$$U_d = k_d \cdot U_{d0} \quad (23)$$

$$\delta = \frac{p}{p_0} \frac{T_0}{T} \quad (24)$$

and the deviation from them are also presented. The breakdown voltages of the experiments are in the range 20 – 160 kV, and it may not be appropriate to apply the same correction throughout this interval. Thus, the results presented in the following sections have been adjusted according to the calibration in the following manner:

- $U < 75$ kV: Reduction of 3.0 kV
- $75 < U < 100$ kV: Reduction of 2.3 kV
- $U > 100$ kV: Reduction of 2.2 kV

Table 1: Calibration of impulse voltage generator by means of a sphere gap

Gap distance [mm]	Breakdown voltage [kV]		Deviation	
	Measured	Table values	[kV]	[%]
20	62.0	59.0	3.0	5.0
30	87.9	85.6	2.3	2.7
40	112.5	110.4	2.2	2.0

3.2 Experimental Method

The 50 % breakdown voltage was found for each gap distance studied by applying positive lightning impulses according to the up and down method described in section 3.2.1. The gap distance (d in Figure 2) was adjusted in steps from 10 mm to 120 mm. For the experiments with an insulating barrier in the gap, gap distance d was fixed at 80 mm while the height of the barrier was adjusted by sliding fasteners on the tubular supports. In this case, the term 'barrier position' refers to the vertical distance between the barrier and the rod tip, denoted d' in Figure 2. Breakdown voltage was measured at four different barrier positions of $d' = 0, 10, 20$ and 40 mm. Barrier positions lower in the gap were not studied as the best performance improvements were expected to be in the upper positions [10]. The barrier was cleaned with isopropyl alcohol between each lightning impulse voltage to eliminate the effect of residual surface charge left from ionisation of the air. An electrostatic voltmeter was used to ensure that the barrier voltage was acceptably low. After an impulse, the electrostatic voltage on the barrier was typically reduced from the range 600 – 1500 V to 0 – 15 V in this way.

Some of the experiments were photographed in order to capture the different breakdown channel paths and the streamer propagation paths during impulses not leading to breakdown. The photographs of breakdown were triggered manually and taken with a long exposure time, typically between 1 and 2.5 s. This means that the images do not necessarily show how the streamers propagated, but only the final breakdown path and other strongly luminous streamers. The faintly luminous streamers present during an impulse resulting in withstand were photographed with a high speed camera in an attempt to observe the streamer behaviour. However, at

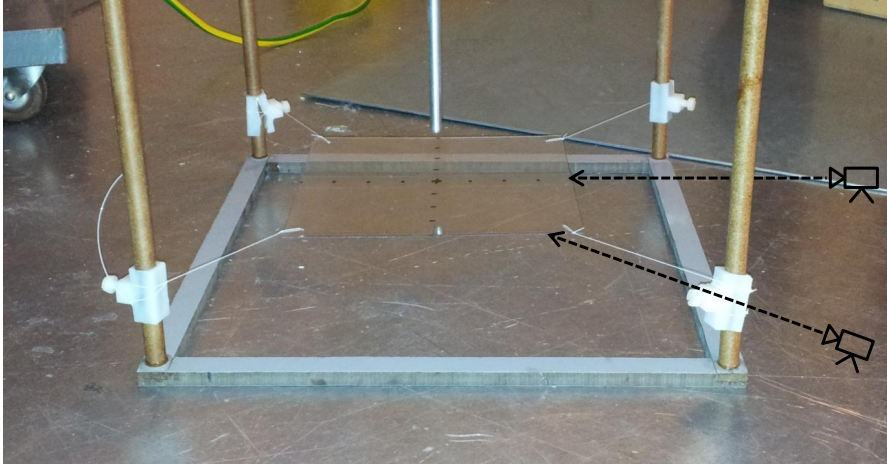


Figure 8: The rod-plane gap arrangement with a 16x16 cm barrier positioned 20 mm from the rod tip. The dashed arrows represent angles of photography.

the desired resolution the camera was only able to record 3800 pictures per second (one frame per $263.16 \mu\text{s}$). At this rate, the streamer will usually be inception, propagate and die all within the time between two frames. A short exposure time would then yield images covering only a short, random interval of time relative to the inception, therefore the maximum exposure time of $240 \mu\text{s}$ was set. A shorter exposure time in addition of a higher frame rate could tell more about exactly where the streamers are inception, but another limitation of the instrumentation would probably come into effect, namely lag in the phosphorescent layer in the image intensifier. The images taken with the intensifier show a lot of glow in the region of the streamers several seconds after the impulse shot. This glow must therefore be attributed to the intensifier itself.

The photographs of the faintly luminous streamers were taken of the 16x16 cm barrier at the two positions of $d' = 20 \text{ mm}$ and 0 mm from the rod tip. In order to get a more precise picture of where the streamers are inception and where they propagate, the images were taken level with the barrier surface and from two different angles, as shown in Figure 8, where the dashed arrows represent the lens axis. A 16x32 cm barrier was also used to determine whether streamers would be inception or propagate on the underside of the barrier. These images were taken parallel to the 32 cm side to avoid the obscuring streamers and get a free view of the space underneath the barrier.

3.2.1 Up and Down Method

This method of conducting a breakdown experiment is mentioned in [1] and [16]. A starting voltage near the true 50 % breakdown voltage is selected and applied to the test object. It is then recorded whether the lightning impulse voltage resulted in breakdown or withstand. If the result was breakdown, the next impulse voltage to be applied is decreased by ΔU . Otherwise, the voltage is increased by ΔU . The recorded voltages will approach the true 50 % breakdown voltage and hover around it, so that over time, the average voltage recorded is equal to the true breakdown voltage U_{50} . The method is illustrated in Figure 9. Best results are obtained when $\Delta U \approx \sigma$ (the standard deviation). An advantage of the up and down method is that it requires few shots compared to other methods with the same level of statistical confidence.

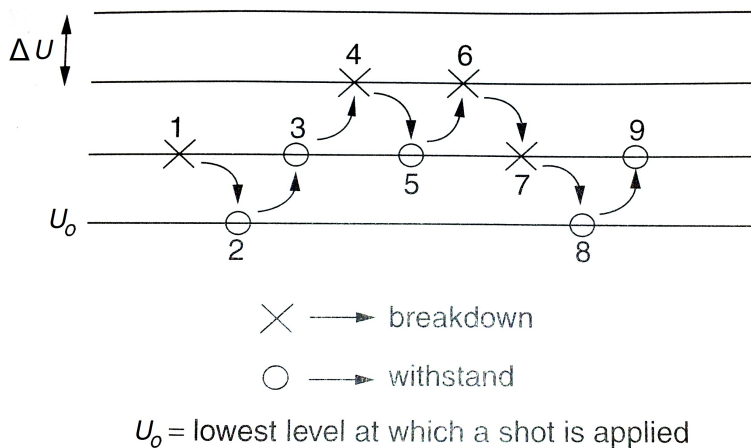


Figure 9: Illustration of the application of the up and down method [1]

In the experiments conducted here the applied charging voltage is adjusted with intervals of $\Delta U = 0.5$ kV, as this was the smallest practically adjustable ΔU . There are five charging capacitors, making the actual $\Delta U = 2.5$ kV.

For determining the breakdown voltage U_{50} the IEC standard requires a minimum of $n = 20$ voltage applications (impulses or shots). In this experiment, 20 applications or more are done for each gap configuration to satisfy this requirement. The obtained data are stored in Excel spreadsheets where the average value and sample variance can be calculated. The readings before a stable up and down pattern is reached (the 'ramp' data) must be omitted when the mean is calculated based on all of the measurements (both withstand and breakdown). If this is done, then the mean is equal to the 50 % breakdown voltage. The sample variance is calculated according to Eq.(25) where n is the number of shots (less the ramp data). The parameter of interest is the standard deviation of the true breakdown voltage, which is not simply $\sqrt{s^2}$ but rather as in Eq.(26) [16]. Here, s is an estimate of the true

σ , only obtainable by conducting an infinite number of experiments.

$$s_{up-down}^2 = \frac{1}{n-1} \left\{ \sum_{i=1}^n U_i^2 - \frac{1}{n} \left(\sum_{i=1}^n U_i \right)^2 \right\} \quad (25)$$

$$s = 1.62\Delta U \left\{ \frac{s_{up-down}^2}{\Delta U^2} + 0.029 \right\} \quad (26)$$

Because the up and down method requires few shots, it is even more important that the measurements be accurate. A pitfall with the method is to choose ΔU too small. Consider Figure 9. For instance, when doing the first measurement quite some distance from the true U_{50} , the ramp up to U_{50} will be long. There is a non-negligible probability that a breakdown will occur during this ramping. In that case the next applied voltage is reduced by ΔU , and this point assumed to be close to the 50 % value. The result can be that the experiment is finished before a sufficient number of readings close to U_{50} is obtained. A symptom of this is a slanted scatter plot. In order to obtain reliable results, scatter plots of each measurement series have been assessed to ensure that the shots are evenly spread around the U_{50} value.

Choosing ΔU too large would also cause problems, as it would lead to readings too far from the 50 % value and give inaccurate results. One must be aware of these pitfalls to get reliable conclusions with the up and down method.

3.3 Field Calculation Using COMSOL

The knowledge of the electric field distribution is necessary to predict where streamers are likely to be incepted and where they propagate. Field calculations can be carried out by computer software such as COMSOL Multiphysics which is used here. The COMSOL software allows for defining the geometry, boundary conditions, materials and so on. By numerically solving the relevant differential equations, information about the electric field can be obtained and graphically presented.

For the purpose of this Master's thesis, COMSOL has been used to calculate the electric field for the rod-plane gap with and without a barrier. The model was parametrized in order to be able to do calculations for different gap spacings and barrier positions quickly. The mesh was refined by custom settings to get accurate results. Field data was extracted from the plot along, for instance, the vertical line from the rod tip down to the grounded plane electrode for use in Matlab.

The simulations have been done on a two dimensional model exploiting the symmetry of the set up. This is a simplification as the barriers used are not disk

shaped, but it is assumed that the simulations are adequately accurate. The model geometry is displayed in Figure 10 (note that the figure is zoomed in versus the model used for simulations). The 7 mm diameter rod is visible to the left, and the barrier is visible in the middle of the gap. The vertical rectangle in the gap is used to refine the mesh extremely fine in this region, while other parts of the model can be more coarsely meshed. The width of the model is 50 cm and the height is the gap distance plus 20 cm. Input to the model includes:

- Ground potential on the bottom plane electrode and the right boundary
- Electric potential on the rod surface
- Electric potential on the upper barrier surface when applicable
- Charge conservation on other surfaces

To simulate accumulated charge on the barrier, the upper surface was given rod potential. Field simulations were also done with streamers propagating along the barrier surface. This was achieved by assigning rod voltage minus the streamer propagation field to the barrier surface within different radii from the rod tip.

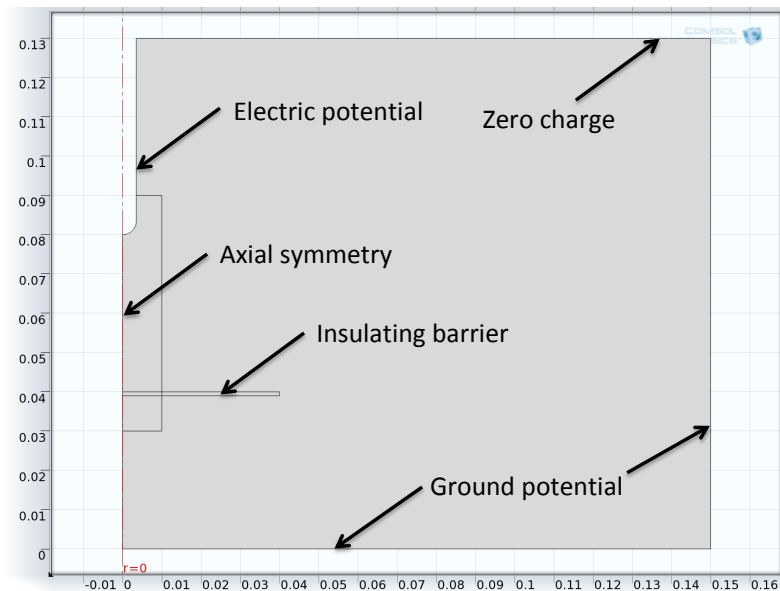


Figure 10: The COMSOL model and its boundary conditions

3.4 Streamer Inception Voltage Calculation Using Matlab

As previously mentioned, field data was extracted from the COMSOL model for further analysis. The COMSOL simulations were conducted with an applied voltage of 15 kV, much lower than the voltage applied in the lab. It is assumed that the field distributions is a function of the geometry and not the voltage itself. Matlab was then used to linearly scale the distributions to the appropriate voltages.

Calculation of the streamer inception voltage was done according to Eqs.(3) and (4). Knowing the field distribution, α_{eff} was calculated for each discrete step and integrated on a straight line from the rod tip to the grounded electrode in the region of $E(x) > 2.5$ kV/mm. The integral yields the value of $\ln(N)$. If the value was not large enough to allow for streamer inception, the voltage was increased, rescaling of the electric field distribution done and the process repeated until the streamer inception voltage was identified through binary search. The Matlab source code can be found in appendix A.

4 Results

4.1 Breakdown Voltage of Rod-Plane Gap

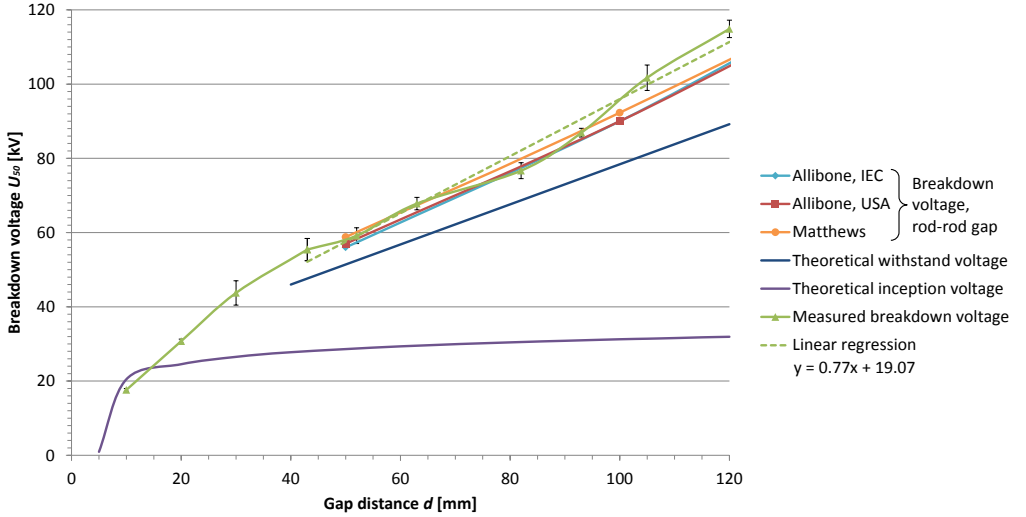


Figure 11: Measured breakdown voltage U_{50} with 99 % confidence interval limits as function of gap distance d [17]. The dashed line represents the linear regression of the results from 43 mm and upwards. Some datasets from literature are included for comparison [18, 19]. In addition, theoretical withstand and inception voltages are plotted.

The experiments have been conducted with positive lightning impulse voltage using the up and down method. For the barrier-less rod-plane gap lightning impulses were applied with 10 different gap spacings d . The measured breakdown voltages and their standard deviations, calculated using Eq.(26), are presented in Table 2 [17]. The results are also presented graphically in Figure 11 by the solid green line with 99 % confidence interval limits as computed using Eq.(13). The purple line is the streamer inception voltage calculated as described in Section 3.4 while the dark blue line represents Eq.(5), the theoretical withstand voltage. The equation is only valid for inhomogeneous fields and the line is therefore not drawn for the smallest gap spacings. With decreasing gap distance, it is observed that the breakdown voltage U_{50} approaches the inception voltage, as expected when the electric field is more uniform (cf. Figure 1). It can be seen that the difference between the predicted withstand voltage and the measured breakdown voltage varies between approximately 7 kV and 26 kV, averaging at 13 kV and increasing with gap distance.

$$U_{50} = 0.77 \text{ kV/mm} \cdot d \text{ mm} + 19.07 \text{ kV} \quad (27)$$

Table 2: Breakdown voltage U_{50} and the standard deviation σ as function of gap distance d , without barrier

Gap distance d [mm]	U_{50} [kV]	σ [kV]
10	17.6	0.4
20	30.8	0.7
30	43.7	5.1
43	55.4	6.5
52	59.2	3.3
63	67.8	2.5
82	76.7	4.1
93	86.9	2.0
105	101.7	7.4
120	114.9	4.1

Linear regression performed on the results yields Eq.(27). The slope coefficient 0.77 kV/mm is quite a bit larger than the streamer propagation field of 0.54 kV/mm defining the slope of the withstand voltage curve. The 99 % confidence interval computed using Eq.(19) for the slope is [0.634, 0.904] kV/mm, which is not wide enough to span the value of 0.54. This can be an indication that the breakdown voltage increases more rapidly than the withstand voltage when lengthening the gap distance, advising for caution when predicting breakdown voltage based on Eq.(5). The constant of 19.07 kV in the linearisation is lower than the 24.4 kV from Eq.(5). Some datasets from literature are included in Figure 11 for comparison, all of them stem from rod-rod gaps with square cross-sectional area of 1.61 cm² [18, 19]. This means that the background field is different and there are also sharper edges on the rods enhancing the field strength. However, the data correspond well with the present results of the rod-plane gap.

4.2 Breakdown Voltage of Rod-Plane Gap with Barrier

Table 3: Measured breakdown voltage U_{50} and standard deviation σ as function of distance d' between rod tip and barrier for the small barriers. Gap distance $d = 80$ mm.

Barrier position d'	4x4 cm		6x6 cm		8x8 cm		
	U_{50}	σ	U_{50}	σ	U_{50}	σ	
40 mm	83.1	4.7	85.4	6.6	86.1	3.0	kV
20 mm	83.0	3.9	84.1	4.0	88.2	2.2	kV
10 mm	76.1	2.6	82.1	3.2	85.2	2.1	kV
0 mm	64.4	4.7	69.5	2.6	72.3	3.0	kV

The impulses were applied to the rod-plane gap fixed at gap distance $d = 80$ mm

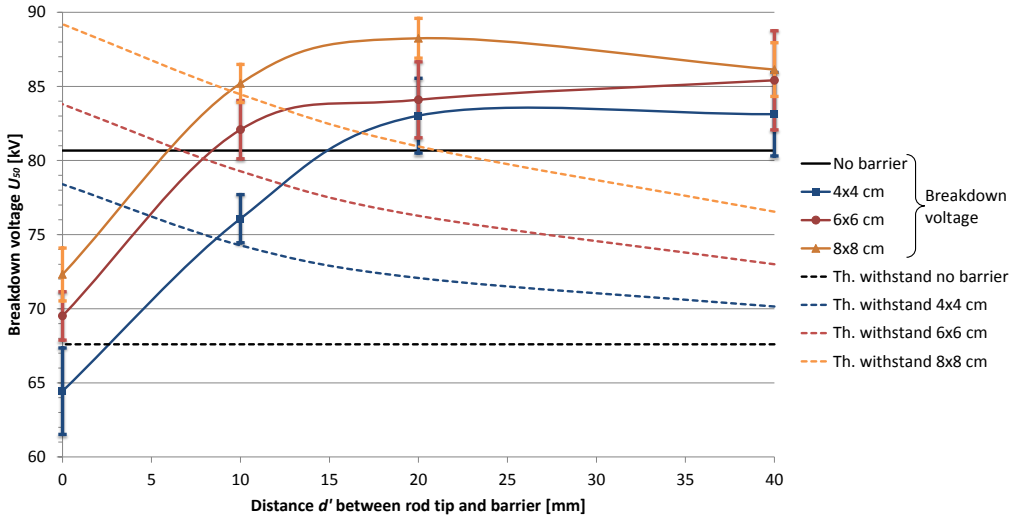


Figure 12: Measured breakdown voltage U_{50} with 99 % confidence interval limits as function of distance d' between rod tip and barrier for the small barriers [17]. Gap distance $d = 80$ mm. Dashed lines show predicted withstand voltages.

with barriers of different sizes mounted at various positions in the gap. The experiments are presented in two groups, the small barriers (4x4 cm, 6x6 cm and 8x8 cm) and the large barriers (16x16 cm, 30x30 cm and 40x40 cm).

For the smaller barriers, the breakdown voltages obtained for the different barrier positions are presented graphically in Figure 12 together with their respective 99 % confidence interval limits, as calculated using Eq.(13). The breakdown voltage of the barrier-less gap is 80.7 kV and is represented by the black horizontal line in the figure. In Table 3 the same values are given in tabular form with the standard deviation as computed using Eq.(26). Predicted withstand voltage levels, as calculated by combining Eqs.(5) and (7), are also plotted in Figure 12 as dashed lines to see whether this can provide any prediction of the breakdown voltage. Although withstand voltage is not equal to the breakdown voltage as such, as already shown in Figure 11, the dashed lines indicate the expected trend when experimenting with different barrier positions d' and sizes in the gap. The difference between withstand and breakdown voltage for the 80 mm gap without the barrier is 13.1 kV. For the $d' = 40$ mm position, the breakdown voltages are approximately equal to withstand voltage plus the mentioned 13.1 kV. As the barriers are moved closer to the high voltage rod, this is no longer true. For the closer positions of $d' = 10$ mm and 0 mm the breakdown voltage drops considerably, even to levels below that of the barrier-less gap. The optimal placement of the small barriers seems to be in the region $d' = 20 - 40$ mm, or expressed by the gap ratio $\frac{d'}{d} = 0.25 - 0.50$. Literature suggests $\frac{d'}{d} = 0.15 - 0.30$ [8]. The highest breakdown

voltage increase achieved with the small barriers is 9.3 % with the 8x8 cm barrier at $d' = 20$ mm.

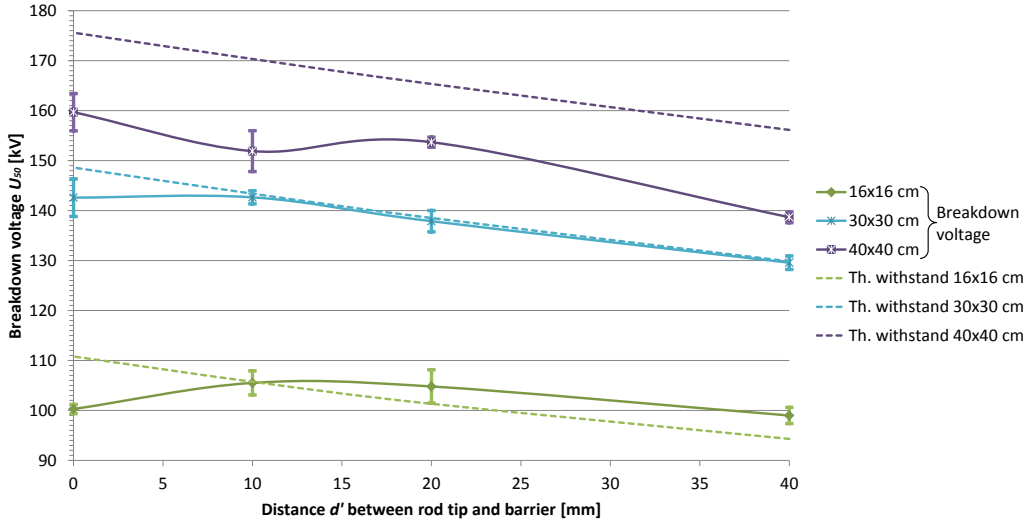


Figure 13: Measured breakdown voltage U_{50} with 99 % confidence interval limits as function of distance d' between rod tip and barrier for the large barriers. Gap distance $d = 80$ mm. Dashed lines show predicted withstand voltages.

Measured breakdown voltages with the larger barriers are presented in Figure 13 with 99 % confidence intervals. Predicted withstand voltage levels are plotted as dashed lines. The results show some of the same trend as seen with the smaller barriers, where a significant breakdown voltage drop was observed for the upper barrier positions. Breakdown voltage for the gap with the 16x16 cm barrier does drop at the upper position, but a level above the breakdown voltage of the barrier-less gap is maintained. For the 30x30 cm barrier there is no drop in breakdown voltage at this position, which may indicate that the mechanism responsible for the decrease is balanced out by the sheer size of this larger barrier. Indeed, with the largest barrier the highest breakdown voltage is obtained at the upper position. It seems that the barrier should be of considerable size compared to the gap length to perform acceptably at all positions. The optimal position varies with barrier size. A position between $d' = 10 - 20$ mm appears to be optimal for the 16x16 cm barrier, equivalent to a ratio of $\frac{d'}{d} = 0.125 - 0.25$. The 30x30 cm barrier displays an increasing breakdown voltage trend with higher positions in the air gap, but levels off at the two upper positions. There is apparently a down swing in breakdown voltage at $d' = 10$ mm for the 40x40 cm barrier, with higher U_{50} to both sides. It should be noted that the 99 % confidence interval is quite wide for this particular measurement. By considering the upper limit of the $d' = 10$ mm measurement and the lower limit of the $d' = 0$ mm measurement, the trend is actually quite

flat, like that of the 30x30 cm barrier. It does seem like the optimal position is $d' = 0 - 10$ mm for the two largest barriers, corresponding to a ratio $\frac{d'}{d} = 0 - 0.125$.

Table 4: Measured breakdown voltage U_{50} and standard deviation σ as function of distance d' between rod tip and barrier for the large barriers. Gap distance $d = 80$ mm.

Barrier position d'	16x16 cm		30x30 cm		40x40 cm		
	U_{50}	σ	U_{50}	σ	U_{50}	σ	
40 mm	99.0	2.5	129.6	2.1	138.7	2.0	kV
20 mm	104.8	6.0	137.9	3.8	153.7	1.6	kV
10 mm	105.5	3.9	142.6	2.0	151.9	6.8	kV
0 mm	100.3	1.4	142.6	8.0	159.7	4.8	kV

It should be noted that the results of the 40x40 cm barrier possibly are affected by the cut-away corners, lowering the breakdown voltage. The results with the larger barriers are also given in tabular form in Table 4 with calculated standard deviation. Note that the standard deviation of some of the measurements are quite large, especially for the 40x40 cm barrier at positions $d' = 10$ mm and 0 mm. The voltages are in the upper range of what the impulse generator can deliver, and the failure of a resistor in the impulse generator limited the number of shots to 15 for the 40x40cm barrier at the upper position $d' = 0$ mm. Normally, at least 20 shots were applied in accordance with Section 3.2.1.

A trend that was not observed with the small barriers but appears in Figure 13, is that increasing barrier size does not match the expected increase in breakdown voltage. With the two largest barriers, the breakdown voltage is actually lower than the withstand voltage prediction of Eq.(5). It is possible that the experiments with the two largest barriers are approaching a limit of the air gap beneath the barrier. As charges are spread over the barrier surface, the field underneath the barrier is increasingly uniform, which means that the inception voltage may again define withstand, cf. Figure 1. According to the slope of 2.6 kV/mm in the figure, a 40 mm air gap of uniform field would see streamer inception at 104 kV. Adding voltage drop of the streamer, for instance for the 30x30 cm barrier in the $d' = 40$ mm position, of $0.54\text{kV/mm} \cdot \sqrt{40^2 \cdot 15^2} \text{ mm} = 23.1 \text{ kV}$ gives a total withstand voltage of 127.1 kV. Compared to the breakdown voltage U_{50} of 129.6 kV this is somewhat optimistic.

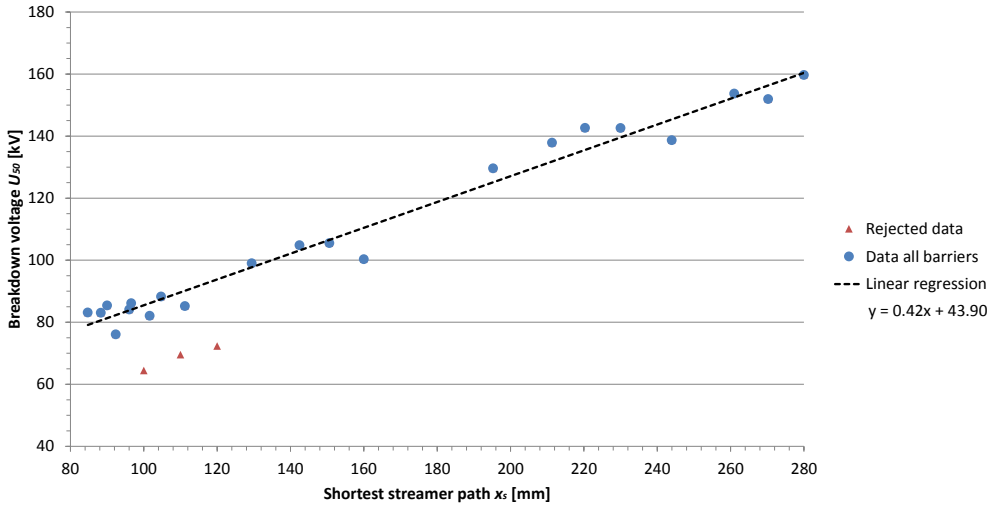


Figure 14: Measured breakdown voltage U_{50} for all the barriers as function of the shortest streamer path x_s as calculated using Eq.(7). Gap distance $d = 80$ mm.

$$U_{50} = 0.42 \text{ kV/mm} \cdot x_s \text{ mm} + 43.9 \text{ kV} \quad (28)$$

Figure 14 shows an attempt to give a better prediction of the breakdown voltage based on all the results obtained with barriers. Linear regression yields the formula given in Eq.(28) where x_s is determined by the gap distance, barrier size and barrier position using Eq.(7). The data from the barrier-less gap is not included as it demonstrates a much steeper slope (cf. Figure 11) of 0.77 kV/mm . The significant difference in slope indicates that introducing a barrier in the rod-plane gap is not equivalent to increasing the gap size to the distance x_s calculated using Eq.(7). The relation between x_s and breakdown voltage seems to be fairly linear and could offer a good prediction when barrier size and position is known. Note that the data points of $d' = 0$ mm for the three smallest barriers have been omitted as they seem to be victim of a mechanism that does not appear to the same extent for the larger barriers. Thus, it must be emphasized that the suggested linear prediction is not valid for these configurations, but is limited to large barriers or small barriers placed in the region $\frac{d'}{d} = 0.125 - 0.50$.

4.3 Streamer Photography

Figure 15 shows two examples of different breakdown channels. The images do not tell where streamers were incepted or exactly how they propagated, but by the assumption that the breakdown channel must succeed a streamer, the pictures

show that streamers can propagate in the air over the barrier and also on the barrier surface. The difference in path length between the two pictures is minimal when the barrier is as large as depicted (30x30 cm). Another observation to be noted is that the breakdown channel is deflected downwards as soon as the barrier edge is reached. The images of Figure 16 were taken to see whether the streamers would tend to go through the cut-out corners of the 40x40 cm barrier or not. Of nine recorded shots, the breakdown channel went through the cut-away corners six times. This can indicate that the breakdown voltage of the barrier is lower than intended because the streamers have a higher probability to reach an end of the barrier. Thus, it behaves more like a disk barrier. Notice the several luminous paths that accompany the breakdown channel in the images of Figures 15b, 16a and 16b.

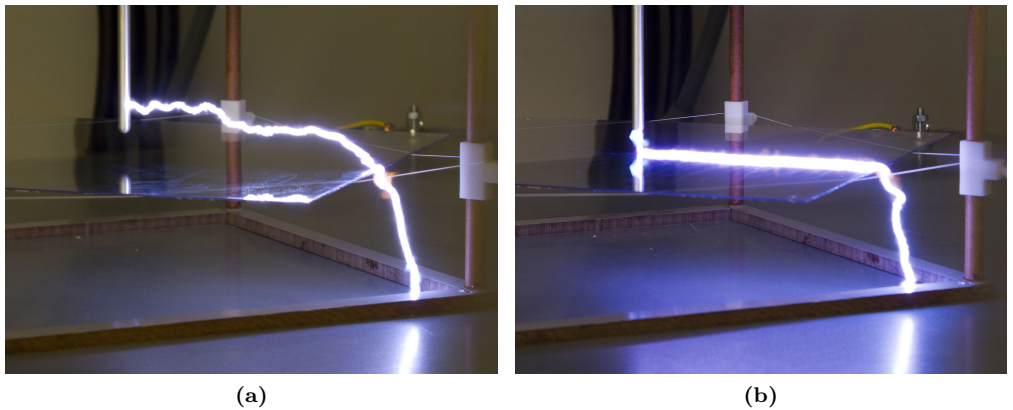


Figure 15: Breakdown channels in 80 mm air gap with 30x30 cm barrier. Applied voltage 146 kV.

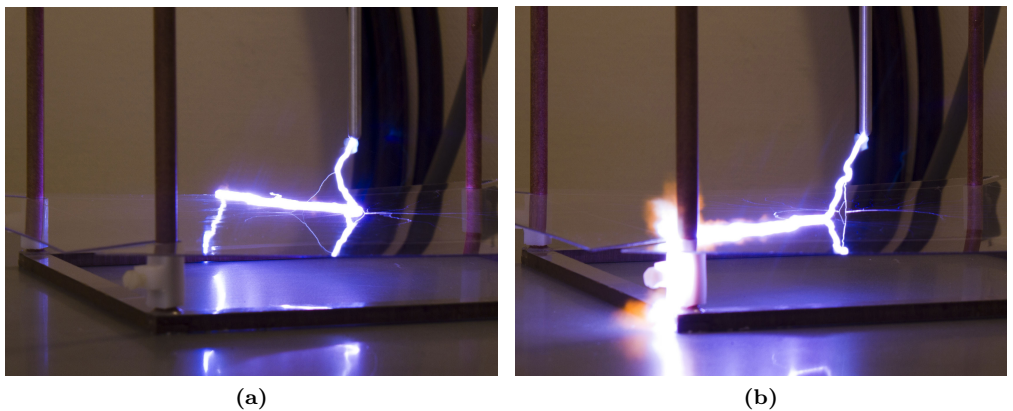


Figure 16: Breakdown channels in 80 mm air gap with 40x40 cm barrier. Applied voltage 141.7 kV.

The streamer phenomena taking place before a breakdown channel is formed are of interest when it comes to understanding where the streamers are incepted and how they propagate. Figure 17 contains three pictures of the rod-plane gap with a barrier where a lightning impulse voltage was applied but breakdown did not occur. The breakdown voltage of the gap depicted is $U_{50} = 104.8$ kV (cf. Table 4) while the applied lightning impulse voltage is 84 kV. A lot of streamer activity is observed even at this level, which means that the inception voltage must be lower than 84 kV. Note that the exposure time of 240 μ s is quite long compared to the duration of the observed phenomena, meaning that the images are cumulative and not instantaneous.

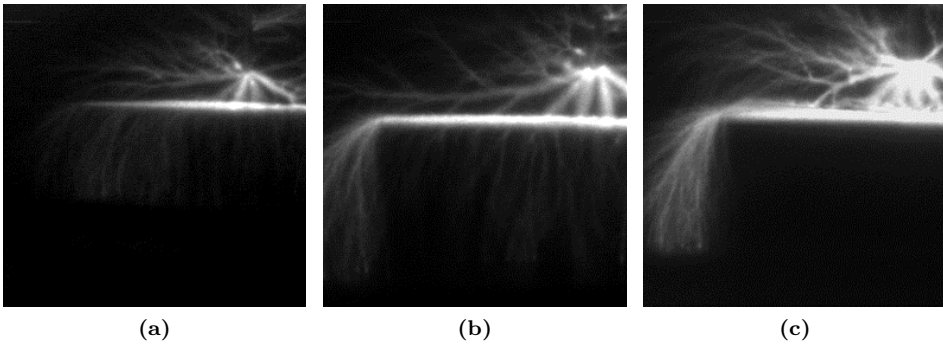


Figure 17: Streamers on the 16x16 cm barrier photographed at an impulse voltage of approx. 84 kV. Gap distance $d = 80$ mm, distance between rod tip and barrier $d' = 20$ mm. In (a) the picture is taken at one of the barrier corners, while in (b) and (c) the lens axis is perpendicular to the barrier edge. The barrier of (c) is 16x32 cm and the picture is taken at the 16 cm side.

Figure 17a is taken along the diagonal of the barrier (recall Figure 8) and shows that there is heavy activity around the rod tip with streamers seemingly propagating in all directions. It is possible to see that the streamers propagate along the surface of the barrier and stretches down towards the ground electrode. It seems that the streamers avoid the corners of the barrier and rather choose the shorter path from the rod tip to one of the barrier edges. Streamer inception is not observed to take place on the barrier corners.

To get a better image of streamer behaviour at the edges, photographs were also captured perpendicular to one of the barrier edges, as the picture in Figure 17b. It shows how the streamers propagate from the rod tip, along the barrier surface and in the air above it, and how they flow over the outer edges and downwards. The streamer approximately 1 cm over the barrier seems to be quite strong and demonstrates that streamers may just as well propagate in the air as on the barrier surface. It is not clear which path a possible breakdown channel would take. Figure 17c shows a special barrier used only for the purpose of this picture. It

measures 16x32 cm and the picture is taken at the shorter side to avoid streamers obscuring the view of the space underneath the barrier. The images of this barrier do not reveal any activity on the underside of the barrier.

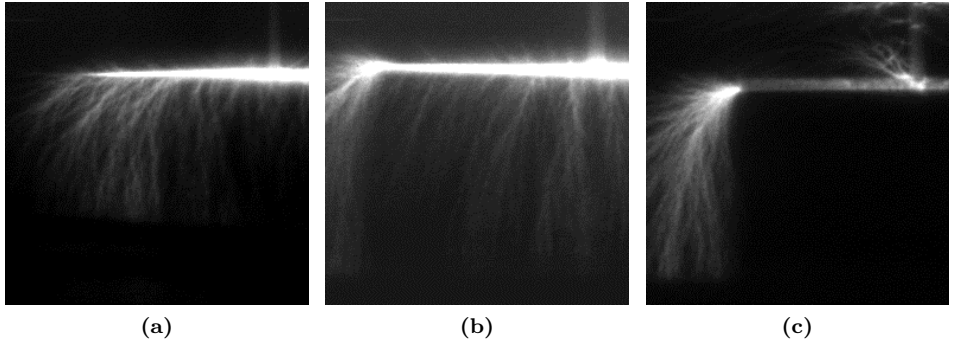


Figure 18: Streamers on the 16x16 cm barrier photographed at an impulse voltage of approx. 84 kV. Gap distance $d = 80$ mm, distance between rod tip and barrier $d' = 0$ mm. In (a) the picture is taken at one of the barrier corners, while in (b) and (c) the lens axis is perpendicular to the barrier edge. The barrier of (c) is 16x32 cm and the picture is taken at the 16 cm side.

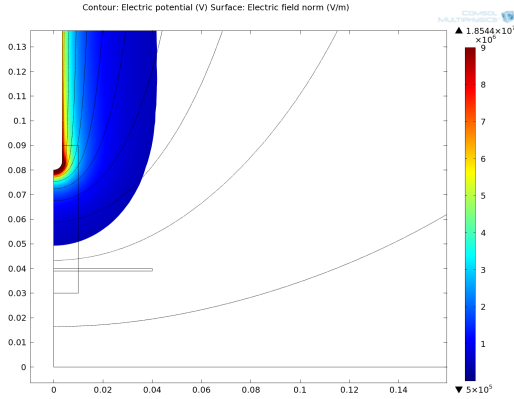
Photographs were also taken of the barrier in its upper position $d' = 0$ mm and can be seen in Figure 18. The breakdown voltage of the gap depicted is $U_{50} = 100.3$ kV (cf. Table 4) while the applied lightning impulse voltage is 84 kV. The photo of Figure 18a is taken along the diagonal and shows little activity along this axis, offering no support to the theory that streamers would be incepted on the underside of the barrier in this position. In contrast to the photographs of Figure 17, streamers do not seem to propagate in the air, but to a much greater extent on the barrier surface only. The photo of Figure 18b is taken perpendicular to one of the edges. It is hard to see whether the streamers propagating down from the barrier originate under the barrier or not. The barrier is strongly illuminated by the streamer activity on the surface, the brightest areas being the centre of the barrier and at the edges. In the picture of Figure 18c there is no visible activity on the underside of the 16x32 cm barrier. Even with the strong electric field, it seems that streamers are still incepted on the rod only. As in Figure 17, streamers can be seen to propagate not only from the tip of the rod, but also from other spots at the rod. In all, the images of Figures 17 and 18 do correspond to the breakdown paths seen in Figures 15 and 16.

4.4 Electric Field Simulation and Inception Voltage Calculation

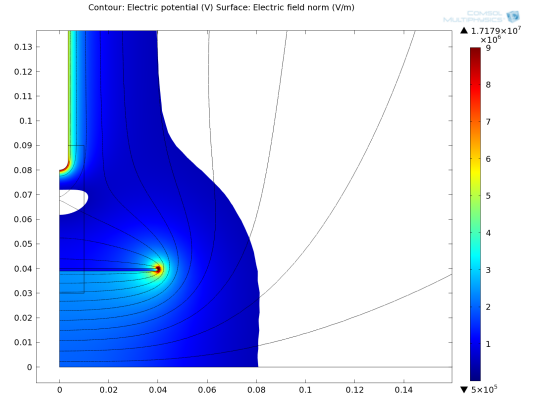
Several different field distributions have been calculated with COMSOL. Figures 19a and b show the field distributions of the 80 mm air gap with the 8x8 cm barrier in the middle of the gap. Applied voltage is 86.1 kV, equal to the measured breakdown voltage of this arrangement. The coloured surface plot indicates field strength, with the maximum value shown on top of the colour legend in each plot. Area with field values below 0.54 kV/mm (the streamer propagation field) is white and marks the region where streamers will not propagate. The left plot shows the background field when the rod is charged with the measured breakdown voltage. The barrier does not seem to impose any substantial distortions of the field. This background field ceases to be valid when a positive space charge is formed near the rod tip, and later when these charges are accelerated downwards and accumulated on the barrier. Assuming that this can be simulated by assigning rod voltage to the barrier surface [8], the resulting field will look more like that of Figure 19b. The field is now strong enough to support streamer propagation across the gap.

Figures 19c and d depict the field distribution when the barrier is positioned close to the high voltage rod tip. Comparing Figures 19a and c, it can be seen that the maximum field strength is increased in the latter case, even though the applied voltage is lowered to 72.3 kV, which is the breakdown voltage for this configuration. The point of maximum field strength is wedged between the rod tip and the barrier, but the field is also enhanced under the barrier, as the permittivity of the barrier will distort the field and give a slightly higher field strength. Again, this is the initial background field. When charged with rod voltage, the field takes the form of Figure 19d.

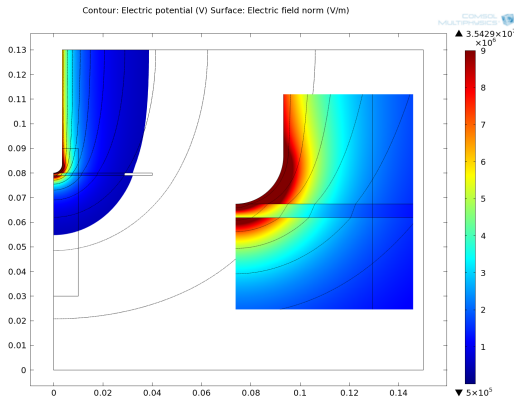
The streamer propagation field of 0.54 kV/mm, or the internal field of the streamer, is the background field necessary to support propagation. Figure 20 displays how the electric field changes when the streamers propagate from the rod tip and outwards. This is simulated by charging the barrier surface with rod voltage minus the propagation field within the radii of 20 mm (20a), 40 mm (20b), 60 mm (20c) and 80 mm (20d). An increasing part of the gap can support streamer propagation as the radius is increased. This shows how the streamer acts like an extension of the high voltage rod, increasing the dielectric stress of the remaining part of the gap. The voltage applied to the rod is 84 kV, equal to the voltage applied in Figures 17 and 18. The point of maximum field strength is again wedged between the rod tip and the barrier, which is probably not realistic as the streamers bridge this small gap. It can be observed that the field under the barrier is increasingly uniform as the streamers propagate along the barrier surface. Figure 21 displays how the electric field strength changes on the underside of the barrier as the charge radius is changed. The maximum point is moved outwards and weakened as the streamer propagates outwards. If inception initially happens at the rod tip, the field on the underside of the barrier may be weakened so rapidly that there will be no visible streamer activity there, as Figures 17c and 18c indicate.



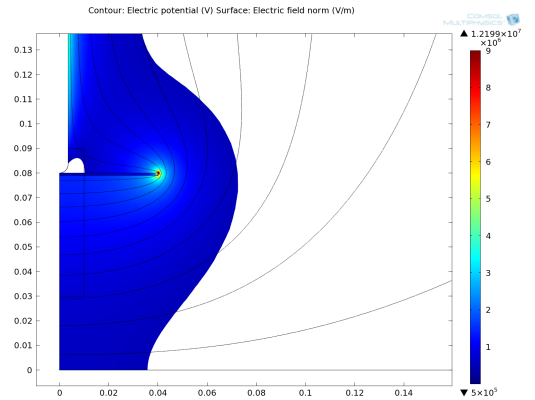
(a) Equipotential lines (black) and colour-graded background field distribution of rod-plane gap with 8x8 cm barrier, $d' = 40$ mm, $U = 86.1$ kV. Area with $E < 0.54$ kV/mm (the streamer propagation field) is white.



(b) Equipotential lines (black) and colour-graded field distribution of rod-plane gap with 8x8 cm barrier, $d' = 40$ mm, $U = 86.1$ kV. The barrier is charged with rod voltage. Area with $E < 0.54$ kV/mm (the streamer propagation field) is white.

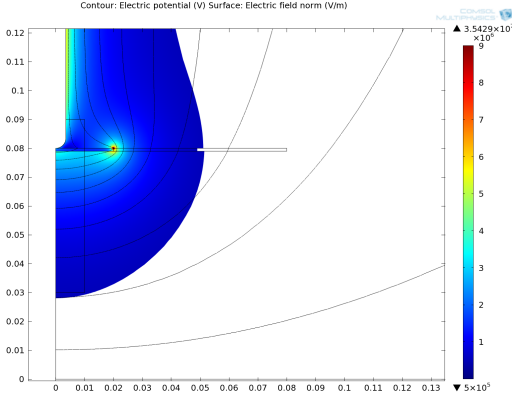


(c) Equipotential lines (black) and colour-graded background field distribution of rod-plane gap with 8x8 cm barrier, $d' = 0$ mm, $U = 72.3$ kV. Area with $E < 0.54$ kV/mm (the streamer propagation field) is white.

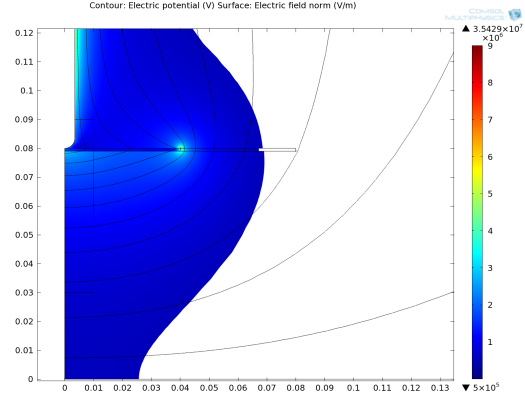


(d) Equipotential lines (black) and colour-graded field distribution of rod-plane gap with 8x8 cm barrier, $d' = 0$ mm, $U = 72.3$ kV. The barrier is charged with rod voltage. Area with $E < 0.54$ kV/mm (the streamer propagation field) is white.

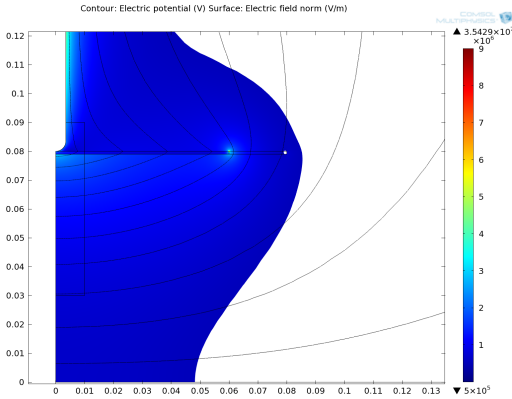
Figure 19: COMSOL electric field surface plots, barrier charged with rod voltage in (b) and (d).



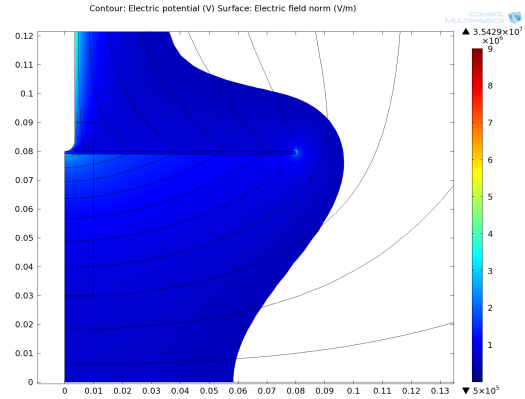
(a) Equipotential lines (black) and colour-graded field distribution of rod-plane gap with 16x16 cm barrier, $d' = 0$ mm, $U = 84$ kV. The barrier is charged with rod voltage minus the propagation field $E = 0.54$ kV/mm in a radius of 20 mm. Space where $E < 0.54$ kV/mm is white.



(b) Equipotential lines (black) and colour-graded field distribution of rod-plane gap with 16x16 cm barrier, $d' = 0$ mm, $U = 84$ kV. The barrier is charged with rod voltage minus the propagation field $E = 0.54$ kV/mm in a radius of 40 mm. Space where $E < 0.54$ kV/mm is white.



(c) Equipotential lines (black) and colour-graded field distribution of rod-plane gap with 16x16 cm barrier, $d' = 0$ mm, $U = 84$ kV. The barrier is charged with rod voltage minus the propagation field $E = 0.54$ kV/mm in a radius of 60 mm. Space where $E < 0.54$ kV/mm is white.



(d) Equipotential lines (black) and colour-graded field distribution of rod-plane gap with 16x16 cm barrier, $d' = 0$ mm, $U = 84$ kV. The barrier is charged with rod voltage minus the propagation field $E = 0.54$ kV/mm in a radius of 80 mm. Space where $E < 0.54$ kV/mm is white.

Figure 20: COMSOL electric field surface plots, barrier charged with streamer voltage.

Inception voltages based on the 16x16 cm barrier surface electric field have been calculated according to Section 3.4 and they are presented in Table 5. The two barrier positions match those of the photographs in Figures 17 and 18, where streamers are clearly being incepted at an impulse voltage of 84 kV. The table

shows that streamers can be incepted on both the upper side and the underside of the barrier in the upper position ($d' = 0$ mm) at this voltage level. The inception voltage is higher when only the tangential field is considered, which is natural as the tangential field is always less than or equal to the absolute value of the field. When considering the absolute field strength, the inception voltage on the top barrier surface is lower than any of the calculated inception voltages on the underside, suggesting that inception will happen more easily on the upper side. For the lower barrier position of $d' = 20$ mm the simulation returns very high inception voltages, an indication that streamers are incepted on the rod rather than on the barrier surface. Note that these inception voltages are virtually the same for all the barriers, because the main part of the electric field is concentrated close to the rod tip. The electric field is weak along the extended integration path gained when increasing barrier size, giving a negligible contribution to the inception integral of Eq.(3). The inception voltage for the vertical path down from the rod tip is presented in Table 6, confirming the theoretical possibility of inception underneath the barrier at 84 kV.

Table 5: Streamer inception voltages calculated on the basis of the background field horizontally along the barrier surface for two different barrier positions, considering both tangential and absolute electric field and with two different integration paths. 16x16 cm barrier, gap distance $d = 80$ mm.

Electric field considered Barrier position	Tangential		Absolute value	
	$d' = 0$ mm	$d' = 20$ mm	$d' = 0$ mm	$d' = 20$ mm
Upper side	56.0 kV	1184.1 kV	17.9 kV	476.3 kV
Underside	78.9 kV	1216.0 kV	40.9 kV	522.7 kV

Table 6: Streamer inception voltages calculated on the basis of the background field vertically down from the rod tip. Gap distance $d = 80$ mm.

16x16 cm barrier, $d' = 0$ mm	41.7 kV
No barrier	31.7 kV

Figure 22 shows the background tangential field on the 4x4 cm, 8x8 cm and 30x30 cm barriers when the respective breakdown voltage is applied. An observation that may be important is that the tangential field covers a larger portion of the barrier surface for the small barriers compared to the larger ones. For instance, the background tangential field strength is above the streamer propagation field for almost the entire 4x4 cm barrier surface at breakdown voltage U_{50} . This can be seen in the figure at the interception between the black and the green lines. With the 8x8 cm barrier, 62 % of the surface is covered, while only 28 % of the surface is covered with the 30x30 cm barrier.

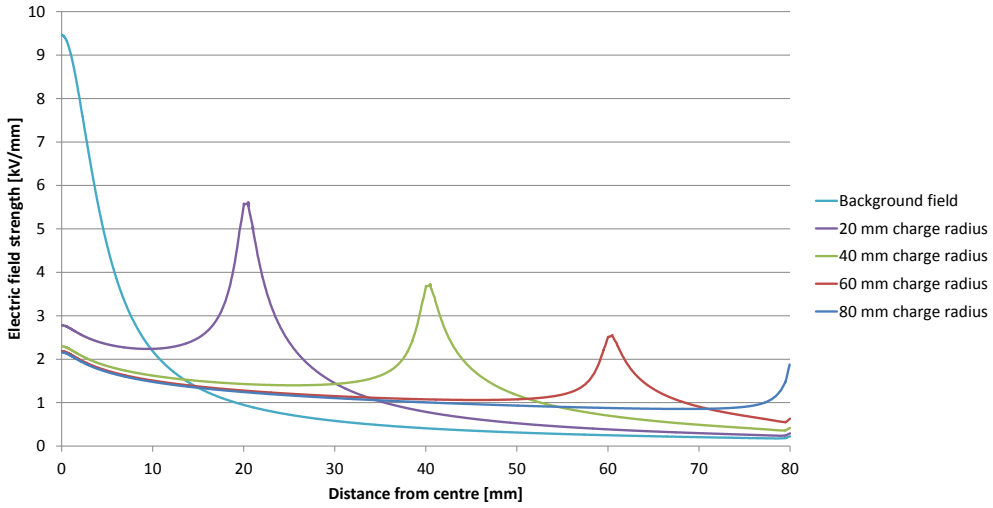


Figure 21: Absolute value of electric field on the underside of the 16x16 cm barrier with different radii of streamer voltage (84 kV rod voltage minus streamer propagation field of 0.54 kV/mm) corresponding to Figure 20. In addition, the original background field is included. Gap distance $d = 80$ mm, distance between rod tip and barrier $d' = 0$ mm.

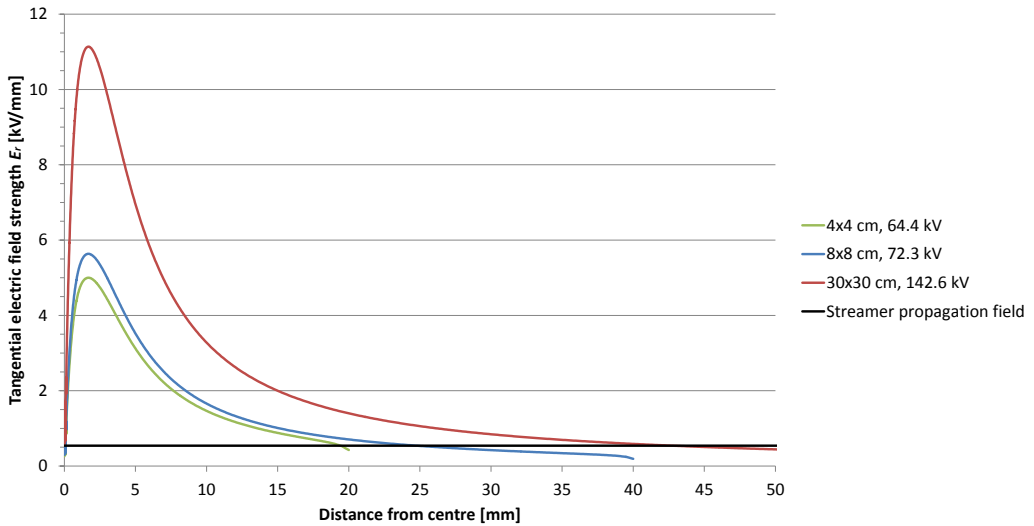


Figure 22: Background tangential electric field strength E_r on the upper barrier surface of the 4x4 cm, 8x8 cm and 30x30 cm barriers at their respective breakdown voltages. Gap distance $d = 80$ mm, distance between rod tip and barrier $d' = 0$ mm.

5 Discussion

5.1 Rod-Plane Gap

The measured breakdown voltages of Figure 11 for the rod-plane gap correlate well with the data from rod-rod gaps, despite their dissimilarities. In addition to the difference in background electric field distribution, the rods are also substantially different. A cylindrical rod with cross-sectional area of 0.385 cm^2 with a rounded tip has been used in the experiments conducted here, while square 1.613 cm^2 cross-sectional rods were used in the rod-rod experiments referred to. The differences advise for caution in attaching importance to the comparison. The rod-rod gaps have a larger number of points of high field stress, which should result in a lower inception voltage. It could therefore be expected that the correlation would not be as good as seen here. However, the main mechanisms behind breakdown are the same for the two gap configurations. They both feature inhomogeneous electric fields and the streamer is incepted on the rod, at least for positive lightning impulses. For the larger gap spacings $d > 100 \text{ mm}$, the measured breakdown voltages increase to somewhat higher levels than for the rod-rod gap.

Breakdown voltage is higher than the theoretical withstand voltage at all gap distances, as should be expected. For the smaller gaps, the breakdown voltage approaches the streamer inception voltage, which is in agreement with theory as the field is more uniform for smaller gap distances [7]. The slope of 0.77 kV/mm of the linearisation curve indicates a higher propagation field than the proposed 0.54 kV/mm . The line is lifted by the two last data points at 105 mm and 120 mm , which have slightly larger standard deviations than the average measurement. The 99 % confidence interval for the steepness does however not contain the proposed value of 0.54 kV/mm , an indication that should not be disregarded. The propagation field of 0.54 kV/mm may be enough to fuel the advance of the streamer, but not enough to cause breakdown, for which it seems that a higher field strength is required. There must be a certain degree of streamer activity to cause breakdown, the event of streamers bridging the gap does not necessarily lead to breakdown, it does only determine the withstand voltage U_W of Eq.(5). The constant of 19.07 kV in the linearisation is lower than the 24.4 kV from Eq.(5). This can not be considered to be important as Eq.(5) is not valid in the region of small gap distances, and the linearisation is not based on the measurements of the small gaps either. The field is more homogeneous in the small gaps, so that the inception voltage is a more correct prediction.

The results indicate that one may not simply compute the mean difference between withstand and breakdown voltage and attribute this difference to other gap spacings. It is reasonable that the extra voltage needed for breakdown is not a constant, like the mean difference of 13 kV , but rather proportional to the gap distance, hence a coefficient larger than 0.54 kV/mm in the linearisation.

5.2 Rod-Plane Gap with Barrier

The results confirm that an increase in breakdown voltage is possible by introducing barriers in the rod-plane gap. At the same time, results demonstrate that placing barriers too close to the high voltage rod tip can be disadvantageous. This is evident in Figure 12, which shows that the breakdown voltage is actually lower than for the barrier-less gap when the barriers are moved to the upper positions. When the small barriers are placed in the middle of the gap, the increase in breakdown voltage is approximately equal to the predicted withstand voltage of Eq.(8) plus 13.1 kV - the difference between withstand voltage and breakdown voltage for the barrier-less 80 mm gap. A reasonable hypothesis could be that the increase in breakdown voltage by moving the barriers and changing their size should match that of the predicted withstand increase due to the longer streamer path. In this way a breakdown prediction is simply made by adding the calculated 13.1 kV difference to the withstand voltage predictions. Figure 12 contradicts this hypothesis for barrier positions $d' < 20$ mm. Breakdown voltage is decreased when the barriers are moved closer to the rod tip, even though the shortest streamer path x_s has its maximum length at this point, which should result in the highest possible breakdown voltage.

For the middle position of $d' = 40$ mm the observed breakdown voltages of the small barriers are approximately equal to the withstand voltage plus the mentioned 13.1 kV. This can indicate that the field distortion caused by the barrier is not significant in this case, owing the breakdown voltage increase to the longer streamer path. The field plot of Figure 19a displays no major field distortions around the barrier. Another factor that may cause an increase in breakdown voltage is the additional time lag induced by the barrier's physical obstruction of the gap. As indicated by Figure 13 and to some extent by 12 the increase in breakdown voltage does not match the expectations when the barrier size is increased at the $d' = 40$ mm and $d' = 20$ mm positions. There is an undeniable increase in breakdown voltage, but the gap between proposed withstand voltage (dashed lines) and measured breakdown voltage is narrowed as the barrier size is increased, again indicating that the prediction is too optimistic.

For the two upper barrier positions of $d' = 10$ mm and $d' = 0$ mm the results give varying conclusions with barrier size. It is disadvantageous to place any of the three smallest barriers in these positions, as the breakdown voltage is substantially reduced, even to levels below that of the barrier-less gap. A reduction was expected as this has been established by other authors [8, 10], but the reduction seen here is more severe. It should be noted that they used barriers of larger size relative to the ground electrode. In the experiments presented here, the ground electrode is very large in comparison to the barriers. This dimension mismatch may impair the performance of the smaller barriers. However, some results in literature have suggested the same trend as seen here [11].

One mechanism behind the observed breakdown voltage reduction is the strong tangential field present on the barrier surface. Figure 19c does for instance show that

the stress on the barrier is much higher in this position compared to Figure 19a. The stronger tangential field makes it easier for the streamers to propagate along the barrier surface compared to the latter figure, where the background field is almost constant over the surface. It has also been calculated that streamer inception can happen on the underside of the barrier when it is in the upper position, cf. Tables 5 and 6. This could also lower the breakdown voltage. These factors may be the main cause of the breakdown voltage reduction observed for the small barriers in the upper positions. In addition, a barrier position closer to the high voltage rod makes charge accumulation on the surface happen faster and breakdown possible at lower voltages [11]. This can explain that breakdown voltages lower than expected were observed also in the $d' = 10$ mm position.

With the large barriers, results show some different trends. The 16x16 cm barrier follows the tendency of the smaller barriers of deteriorating breakdown performance in the upper position $d' = 0$ mm. However, the two largest barriers do not experience this effect to the same extent. It seems that increasing the barrier size eventually outperforms the mechanisms responsible for the breakdown voltage reduction observed with the small barriers close to the rod tip. The results of the three largest barriers are more in accordance with the conclusions in [10], where only a slight reduction of breakdown voltage is seen in the upper barrier position. The rise in breakdown voltage by increasing barrier size from 30x30 cm to 40x40 cm is maybe not as high as expected. As streamers propagate on the barrier surface, the field on the underside is made more uniform as seen in Figure 20d. It may be expected that a limit in breakdown voltage eventually is reached when increasing the barrier size because of this uniform field. It may not be possible to increase the breakdown voltage indefinitely by just increasing barrier size, as there is a risk of breakdown of the uniform gap under the barrier. However, the results do not give conclusive evidence to claim that this limit is reached in the experiments conducted here.

It has been proposed that the tangential field is a key factor of reducing the breakdown voltage for the small barriers. As Figure 22 demonstrates, the area of high tangential field is reduced relative to the barrier surface when the barrier size is increased. The small barriers are so limited in size that the background tangential field covers the entire or most of the barrier surface already at gap breakdown voltage of $U_{50} = 80.7$ kV. This means that the applied voltage can be reduced while retaining a tangential field strong enough to quickly accelerate charge carriers and charge the barrier. As the barrier size is increased, the tangential field at 80.7 kV will cover less area relative to the barrier surface, requiring a higher voltage to maintain a satisfactory field strength. In addition, the streamer voltage drop of 0.54 kV/mm increases linearly with barrier size, also demanding a higher applied voltage. It seems that the streamer voltage drop is negligible for the small barriers, but as the barrier size is increased, the distance that the streamer must propagate is of greater importance. In addition, the larger barriers do not give the same dimension mismatch as with the small barriers. The results seem to indicate that barriers with a cross-sectional length of twice the gap distance should be used

in order to achieve satisfactory performance improvements.

Optimal barrier position has been claimed in literature to be $\frac{d'}{d} = 0.20$ [10] or in the interval $\frac{d'}{d} = 0.15 - 0.30$ [8]. As can be seen in Figure 13 this is very much supported by the results for the 16x16 cm barrier, having the best performance at $\frac{d'}{d} = 0.125 - 0.25$. Figure 12 demonstrates that the three smallest barriers give the best results at the interval $\frac{d'}{d} = 0.25 - 0.50$, also overlapping the proposed interval. In contrast, the 30x30 cm and 40x40 cm barriers perform the best at the upper positions of $\frac{d'}{d} = 0 - 0.125$ which is closer to the rod than recommended in literature. The breakdown voltage saw an increase of 98.0 % with the 40x40 cm barrier at the upper position, the largest increase achieved. It is in accordance with the results of [10], but not quite as good as in [8], where the breakdown voltage was more than tripled. This particular measurement pushed the impulse voltage generator to its limits, twice resulting in resistor failure in the sphere gap. Only 15 shots were applied in contrast to the recommended minimum of 20. This measurement may therefore be less reliable than the other measurements, although this is accounted for in the calculation of the 99 % confidence interval.

The withstand prediction has been based on Eq.(5), which defines the withstand in a rod-plane gap. Here it is applied assuming that gap length d can be replaced with the shortest streamer path x_s from Eq.(7). This assumption does not seem to be correct (cf. Figures 12 and 13). An explanation is that the electric field is higher in a rod-plane gap with a barrier where $x_s = d$ compared to a plain rod-plane gap of distance d , because the physical distance between the rod tip and the ground electrode is shorter. The higher field strength probably makes breakdown happen more easily. Thus, the results suggest that a rod-plane gap with barrier insulation giving a shortest streamer path x_s is not equal to a rod-plane gap with gap distance $d = x_s$. An empirical formula which offers a better prediction of the breakdown voltage for the gap configurations studied here is given in Eq.(28). Combined with the linearisation in Eq.(27) of the results of the barrier-less gap it can actually be calculated that increasing x_s by for instance 1 cm with a barrier does only give the same performance as increasing the gap distance 0.54 cm in the barrier-less gap.

The photographs of Figures 17 and 18 give no basis to claim that streamers are incepted at the barrier edges or on the underside of the barrier. At the upper barrier position $d' = 0$ mm the streamer inception voltages calculated along the upper barrier surface, the bottom barrier surface and also along the vertical line from the bottom barrier surface down to the ground electrode are all lower than the applied voltage. This should allow streamers to be incepted and propagate from the underside. Yet, this has not been observed. It may be the case that the streamer activity is initiated at the rod tip because of the slightly higher field there. The strong tangential electric field will quickly accelerate any charges away from the rod, leading to a severely weakened field on the underside of the barrier beneath the rod tip, preventing streamer inception there. Instead, the charges close to the rod tip form an avalanche and further weaken the field under the barrier, as seen in Figure 21. There may be discharge activity under the barrier that is not captured by the camera.

It has been observed that the breakdown channels (cf. Figures 15 and 16) sometimes follow the barrier surface and sometimes avoid it completely. It is also seen that there can be several fairly progressed paths extending over the barrier surface at the point of breakdown. This shows the random nature of the streamer propagation path, which can be studied further in for instance Figure 17b. There is a long streamer with branches propagating over the barrier. In the event of a breakdown, it is not clear which channel would end up dominating. What seems more consistent is that the streamers deflect over the barrier edge and turn downwards (cf. Figures 17b, 17c and 18c), which is in line with theory that the streamer tends to follow electric field lines when possible, but at the same time not propagate outside the 0.54 kV/mm region [7]. The field plot of Figure 20d shows that to satisfy this, the streamers must make a sharp turn after reaching the barrier edge (to avoid white space in the figure).

5.3 Sources of Error

Oscilloscope Readings

All the measured voltages were read with the oscilloscope Cursor tool. One clear disadvantage with this method is that the cursors could only be moved in steps of 0.2 V at the relevant zoom level. Converted to gap voltage, this step is 1 kV. This is somewhat coarse. Another disadvantage is that the ΔU of the applied voltage is 2.5 kV, which will then sometimes be read as 2 kV and sometimes as 3 kV. There may not be a sufficient amount of readings to compensate for this extra uncertainty.

Humidity and Temperature

The effects of humidity and temperature have been neglected. It has been assumed that the lab offers relatively stable conditions, but the experiments have been conducted over a long period of time. Thus, the conditions have probably been affected by changing weather. It should be considered to monitor the surrounding conditions more accurately if further work on the subject be done.

Barrier Placement and Residual Charges

Residual charges on the barrier surface left from previous shots distort the electric field and may affect the withstand voltage. By cleaning the barrier between each shot, it is reasonable to believe that this effect has been eliminated here. However, the cleaning itself may change the barrier position and orientation slightly, for instance by loss of tension in the barrier suspension. The barrier position was routinely checked to avoid misplacement.

The positioning of the barrier may also be inaccurate because it was conducted by hand and by use of simple measurement tools.

6 Conclusion

The experiments that have been carried out and presented here do not contradict established theory regarding breakdown voltage in rod-plane gaps. The results of the barrier-less gap show a linear relationship between gap distance and breakdown voltage in the inhomogeneous area, as in line with literature [7]. Linearisation of the results in the inhomogeneous region yields a slope of 0.77 kV/mm, suggesting that a field strength higher than the internal field of the streamer (0.54 kV/mm) is required to cause breakdown with 50 % probability.

Experiments have been conducted with barriers in the mentioned rod-plane gap, fixed at $d = 80$ mm, to investigate to what extent they offer an increase in breakdown performance as literature suggests. For rod-plane gaps with square polycarbonate insulating barriers, the results do not give unequivocal recommendations. The size of the barrier and how it is placed in the gap is of great importance when it comes to achieving a satisfactory performance improvement. As Figure 12 demonstrates, small barriers do only offer a slight increase in the breakdown voltage. An increase of 9.3 % has been achieved here with an 8x8 cm barrier. It seems that barrier size (cross-sectional length) should be twice the gap length or larger to give significant improvements. By employing larger barriers up to 40x40 cm, it has been possible to increase the breakdown voltage by 98.0 %. It has been suggested in literature that a single barrier can triple the breakdown voltage [8].

The results have shown a substantial drop of breakdown voltage when small barriers have been placed close to the high voltage rod tip. This trend has also been suggested by several authors [8, 10, 11]. Caution must therefore be paid to the placement of small barriers, which have shown the best performance in the area $\frac{d'}{d} = 0.25 - 0.50$. In literature the optimal barrier position has been claimed to be $\frac{d'}{d} = 0.15 - 0.30$ [8], which is in accordance with the optimal positions $\frac{d'}{d} = 0.125 - 0.25$ of the 16x16 cm barrier studied here. The largest barriers of size 30x30 cm and 40x40 cm have optimal performance in the region $\frac{d'}{d} = 0 - 0.125$. As can be seen in Figure 13, the larger barriers do not experience the same performance drop at the upper barrier positions experienced with the smaller barriers.

A suggested explanation of the significant breakdown voltage reduction is the strong tangential field present on the barrier surface when it is placed close to the high voltage rod tip. For the small barriers, the background tangential field can support streamer propagation over almost the entire barrier surface. As a streamer is incepted and propagates from the rod tip, the field is enhanced in front of the avalanche head and will further accelerate the streamer over the barrier. The maximum field strength of the gap is slightly increased when the barrier is in the upper position, making discharges happen more easily. The charge carriers do also reach the barrier faster and charge it when closer to the rod [11]. When the barrier is placed at some distance from the rod tip these effects seem to be averted. By increasing barrier size, higher voltage is necessary to maintain satisfactory field strength for streamer propagation. Avoiding the unfavourable configurations men-

tioned, the empirical formula given below can be used to predict the breakdown voltage based on the shortest possible streamer path x_s , defined by gap length, barrier size and barrier position. The results demonstrate through this formula that a rod-plane gap with barrier insulation giving a shortest streamer path x_s does not give a breakdown voltage as high as a rod-plane gap with gap distance $d = x_s$ does.

$$U_{50} = 0.42 \text{ kV/mm} \cdot x_s \text{ mm} + 43.9 \text{ kV}$$

Streamers have been seen to propagate in all directions from the rod tip, cf. Figure 17. Upon reaching the barrier edges, the streamers are deflected downwards, staying within the region where the electric field is higher than the propagation field as claimed in literature [5]. Calculations have supported the possibility of streamer inception on the underside of the barrier when it is positioned in the upper position of the gap. This has however not been observed during the conducted experiments, and is maybe explained by the slightly higher field on the top surface. If discharges initially occur there, the field is weakened on the underside of the barrier, preventing inception.

7 Further Work

The experiments conducted in this Master's thesis have been limited by a number of factors. The barriers have only been tested in the fixed $d = 80$ mm rod-plane gap. It would be of interest to test whether the conclusions and trends from the experiments are transferable to real industrial applications such as breakers. The proposed breakdown voltage prediction of Eq.(28) may not be valid for real applications and further investigation should be done with larger barriers and air gaps. For instance, there may be a limit defined by the withstand voltage of the uniform gap under the barrier, suspending the validity of the proposed prediction formula. Different barrier configuration is another area of interest, the experiments here are for instance done with a single barrier only. A set-up with multiple barriers could give another indication of the validity of the offered breakdown voltage prediction. A cylindrical housing with electrodes at each end with barriers in a zigzag arrangement could for instance be studied. Different barrier material is another parameter of possible interest to examine, in addition to the effect of surface roughness. It should also be considered to improve the COMSOL model used, especially when it comes to modelling the charging of the barrier surface, which has been done here by simply assigning variable voltage to the surface.

The pictures of streamers here were taken with a long exposure time relative to the mechanisms behind the observed phenomena. For further study of where the streamers are incepted and where they propagate, a camera capable of a higher frame rate should be used.

8 References

- [1] E. Kuffel, W. S. Zaengel, and J. Kuffel, *High voltage engineering fundamentals*. Oxford: Butterworth Heinemann, 2nd ed., 2000.
- [2] E. Ildstad, *Electric power engineering: TET4160 High voltage insulating materials*. Trondheim: Department of Electric Power Engineering, NTNU, 2010.
- [3] M. Naidu and V. Kamaraju, *High Voltage Engineering*. New Delhi: McGraw-Hill, 1982.
- [4] F. Mauseth, “Optimalisatie van isolatieconstructie voor 25 kV bovenleidingsysteem,” Master’s thesis, Delft University of Technology, Delft, 2001.
- [5] T. Christen, H. Böhme, A. Pedersen, and A. Blaszczyk, “Streamer line modeling,” in *Scientific Computing in Electrical Engineering*, Mathematics in Industry, Toulouse: Springer Verlag Berlin Heidelberg, 2012.
- [6] K. Petcharak, *Applicability of the streamer breakdown criterion to inhomogeneous gas gaps*. PhD thesis, Swiss Federal Institute of Technology, Zürich, 1995.
- [7] A. Pedersen, T. Christen, A. Blaszczyk, and H. Böhme, “Streamer inception and propagation models for designing air insulated power devices,” in *IEEE Conference on Electrical Insulation and Dielectric Phenomena*, pp. 604–607, October 2009.
- [8] S. Lebedev, O. Gefle, and Y. Pokholkov, “The barrier effect in dielectrics: the role of interfaces in the breakdown of inhomogeneous dielectrics,” *IEEE Transactions on Dielectrics and Electrical Insulation*, vol. 12, pp. 537–555, June 2005.
- [9] A. Kara, O. Kalenderli, and K. Mardikyan, “DC breakdown voltage characteristics of small air gaps with insulating barriers in non-uniform field,” in *International Conference on High Voltage Engineering and Application (ICHVE)*, pp. 425–428, October 2010.
- [10] L. Ming, M. Leijon, and T. Bengtsson, “Factors influencing barrier effects in air-gaps,” in *9th International Symposium on High Voltage Engineering*, pp. 2168–1–2168–4, September 1995.
- [11] F. V. Topalis and I. A. Stathopoulos, “Barrier effect on electrical breakdown in air gaps: A theoretical approach,” in *9th International Symposium on High Voltage Engineering*, pp. 2147–1–2147–4, September 1995.
- [12] R. E. Walpole, R. H. Myers, S. L. Myers, and K. Le, *Probability & Statistics for Engineers & Scientists*. Pearson Prentice Hall, 8th ed., 2007.
- [13] J. T. Kvaløy and H. Tjelmeland, *Tabeller og formler i statistikk*. Trondheim: Tapir akademisk forlag, 2nd ed., 2009.

- [14] E. Ildstad, "Laboratorieoppgave OV2: Generering og fordeling av impulsspenninger," 2008.
- [15] IEC, *Recommendations for Voltage Measurements by Means of Sphere-gaps (one sphere earthed)*. Geneva: IEC Publication 52, 2nd ed., 1960.
- [16] W. J. Dixon and F. J. Massey Jr., *Introduction to statistical analysis*. McGraw-Hill, 3rd ed., 1969.
- [17] J. S. Jørstad, "Effect of barriers in air insulated rod-plane gaps," December 2011.
- [18] T. E. Allibone, "International comparison of impulse-voltage tests," *Journal of the Institution of Electrical Engineers*, vol. 81, pp. 741–750, December 1937.
- [19] J. Matthews and R. Saint-Arnaud, "Characteristics of impulse breakdown of standard rod gaps under controlled-atmosphere conditions," *Proceedings of the Institution of Electrical Engineers*, vol. 118, pp. 1524–1527, October 1971.

A Matlab Source Code

The below Matlab function can be called to find the inception voltage of the given electric field distribution.

```
%The function taks electric field data from a rod-plane gap as input with  
%known applied voltage of 15kV and calculates the inception voltage
```

```
function U = inception(s_original)  
%s_original is a vector with position [m] in the first column and  
%electric field strength [V/m] in the second column  
  
%A while loop is used to increase the voltage until there are  
%enough electrons  
  
U_next = 100; %[V]  
U_prev = U_next;  
electrons = log(10^8);  
done = 0;  
  
while ~done  
    %Scaling the data to a new voltage  
    s = skaler(s_original, 15000, U_next);  
  
    %Calculates the integral of the streamer inception criterion  
    I = integrate_criterion(s);  
  
    %Checking whether there are enough electrons. If not, voltage  
    %is increaseed  
  
    if I>electrons  
        done = 1;  
    elseif U_prev > 8000000  
        disp('Error. Task is aborted.');
```

```
        U = U_prev;  
        return  
    else  
        U_prev = U_next;  
        U_next = U_prev*2;  
        done = 0;  
    end  
end  
  
%A while loop is used to find the inception voltage by binary search  
  
U_upper = U_next;  
U_lower = U_prev;
```

```

done = 0;

while ~done
    U_test = (U_upper + U_lower)/2;

    %Scaling the data to a new voltage
    s = skaler(s_original, 15000, U_test);

    %Calculates the integral of the streamer inception criterion
    I = integrate_criterion(s);

    %Checking whether the test voltage interval has become infinitely
    %narrow, meaning that the inception voltage has been determined

    if floor(U_upper) == floor(U_lower)
        done = 1;
    end

    %Checking whether there are enough electrons

    if I>electrons
        U_upper = U_test;
    else
        U_lower = U_test;
    end
end
U = U_test;
end

```

The below Matlab function can be called to calculate the integral of Eq.(3).

```

%The function calculates the integral of the streamer inception criterion
%for values of the electric field above 2.5 kV/mm

```

```

function I = integrate_criterion(s)

    dim = size(s);          %Returns the number of [rows columns]
    s(:,2) = s(:,2) / 1000000; %Changes unit from V/m to kV/mm
    s(:,1) = s(:,1) * 1000;   %Changes unit from m to mm

    %The for loop sums the effective ionisation coefficient of the
    %electric field data. Petcharakis 1995.

    I=0;

    for i=2:dim(1,1)

```

```

if s(i,2)>2.588 && s(i,2)<=7.943
    step = (s(i,1) - s(i-1,1)); %Calculating step in mm
    I = I + (1.6053*( s(i,2) - 2.165)^2 -0.2873)*step;
elseif s(i,2)>7.943 && s(i,2)<=14
    step = (s(i,1) - s(i-1,1));
    I = I + (16.7766*s(i,2) - 80.0006)*step;
elseif s(i,2)>14
    step = (s(i,1) - s(i-1,1));
    I = I + (1175*exp(-28.38*s(i,2)))*step;
end
end
end

```